KfK 4729
Juni 1994

Chemical Interactions between as-received and pre-oxidized Zircaloy-4 and Inconel-718 at High Temperatures

P. Hofmann, M. Markiewicz
Institut für Materialforschung
Projekt Nukleare Sicherheitsforschung

Kernforschungszentrum Karlsruhe

Kernforschungszentrum Karlsruhe
Institut für Materialforschung
Projekt Nukleare Sicherheitsforschung

KfK 4729

Chemical interactions between as-received and pre-oxidized Zircaloy-4 and Inconel-718 at high temperatures

P. Hofmann, M. Markiewicz*

*Comisión Nacional de Energia Atómica
Av. del Libertador 8250, 1429 Buenos Aires
Argentina

Kernforschungszentrum Karlsruhe GmbH, Karlsruhe

Als Manuskript gedruckt

Kernforschungszentrum Karlsruhe GmbH
Postfach 3640, 76021 Karlsruhe

ISSN 0303-4003

Abstract

Isothermal reaction experiments were performed in the temperature range of 1000 - 1300 °C in order to determine the chemical interactions between Zircaloy-4 fuel rod cladding and Inconel-718 spacer grids of Pressurized Water Reactors (PWR) under severe accident conditions. It was not possible to apply even higher temperatures since fast and complete liquefaction of the components occurred as a result of eutectic interactions during heatup. The liquid reaction products formed enhance and accelerate the degradation of the material couples and the fuel elements, respectively. Only small amounts of Inconel are necessary to liquefy large amounts of Zircaloy.
Thin oxide layers on the Zircaloy surface delay the beginning of the chemical interactions with Inconel but cannot prevent them. In this work the reaction kinetics have been determined for the system: as-received and pre-oxidized Zircaloy-4/Inconel 718. The interactions can be described by parabolic rate laws; the Arrhenius equations for the various interactions are given.

Chemische Wechselwirkungen von Zircaloy-4 im Anlieferungs- und voroxidierten Zustand mit Inconel 718 bei hohen Temperaturen

Zusammenfassung

Zur Bestimmung der chemischen Wechselwirkungen zwischen Zircaloy-4-Brennstabhüllrohren und Inconel 718-Abstandshaltern von Druckwasserreaktoren unter schweren Unfallbedingungen wurden isotherme Reaktionsexperimente im Temperaturbereich 1000 - 1300°C durchgeführt. Höhere Temperaturen konnten nicht angewandt werden, da eine schnelle und vollständige Verflüssigung der Materialien infolge eutektischer Wechselwirkungen schon in der Aufheizphase stattfand. Die entstehenden flüssigen Phasen beschleunigen die weitere Zerstörung der Materialproben bzw. der Brennelemente. Nur geringe Mengen an Inconel sind notwendig, um große Mengen an Zircaloy zu verflüssigen.

Dünne Oxidschichten auf der Zircaloy- Oberfläche verzögern den Beginn der chemischen Wechselwirkungen mit Inconel, sie können jedoch nicht verhindert werden. Im Rahmen dieser Arbeit wurde die Reaktionskinetik für die Systeme nicht oxidiertes Zircaloy/Inconel und voroxidiertes Zircaloy/Inconel bestimmt. Die verschiedenen chemischen Wechselwirkungen können durch parabolische Zeitgesetze beschrieben werden; die Arrheniusgleichungen werden angegeben.

Contents

1. Introduction 1

2. Experimental Details 1

3. Results 2

3.1 Chemical behavior 2

3.2 Reaction kinetics 5

3.3 Influence of an oxide layer on Zircaloy/Inconel interaction 6

4. Discussion 8

5. Summary and Conclusions 9

6. Acknowledgement 10

7. References 10

List of Tables 11

List of Figures 12

1. Introduction

In severe reactor accidents the temperature within the core exceeds 1200°C, which is the maximum tolerable temperature for design-basis accidents. At these high temperatures the various materials of the fuel-rod bundles interact chemically with each other and with the steam of the environment. With respect to core damage initiation and progression, eutectic interactions are of special interest since these interactions result in the formation of liquid phases at low temperatures. Experiments with fuel-rod bundles, which were heated up to 2000°C, clearly showed, by optical observations and temperature measurements, the significant impact of Inconel spacer grids on the early melt formation and damage propagation within the fuel assembly at rather low temperatures [1, 2]. Inconel spacer grids fail due to liquefaction below their melting point (around 1450°C), as a result of eutectic reactions, of nickel and other Inconel alloy components with zirconium. The resulting liquid reaction products relocate and enhance and accelerate the degradation of the fuel rod bundle.

Given this body of evidences, a very important aspect is to study the reaction kinetics and the onset of liquid phase formation between Zircaloy cladding (Zry) and Inconel 718 caused by the chemical interactions.

The Zry cladding was used in the as-received condition and in the pre-oxidized (10, 20, 45, µm oxide layer thicknesses) condition. An oxide layer on the surface of Zry can initially prevent the interaction with Inconel, but the oxide is rapidly dissolved in the Zry at higher temperatures, during an incubation period, t_0. The result of the separate-effects tests are the basis for the description of the material interactions by models which can be used in computer code systems.

2. Experimental Details

The isothermal annealing experiments were performed with Zircaloy-4 (Zry) capsules into which short cylindrical rods of Inconel 718 had been pressed and closed gas-tight by a conical Zry plug. Figure 1 shows the components of a compatibility specimen before being loaded.

The annealing experiments were performed in a tube furnace under flowing

argon. The specimens were heated up to about 900°C and then placed into the pre-heated furnace which had the desired annealing temperature. The annealing time started when the temperature of the specimen was 20 K below the annealing temperature. The specimens were cooled down to room temperature outside the furnace.

The temperatures investigated ranged from 1000 to 1300°C and the maximum annealing time was 300 minutes. The highest temperature which could be examined was determined by the condition of the reaction couple,with limits imposed by the failure of the specimen due to the onset of liquid phase formation followed by a fast and complete liquefaction of the Zry crucible at slightly higher temperatures.

After annealing, the specimens were mechanically cut and then metallographically prepared for examinations of the reaction zones with an optical microscope. Some of the specimens were etched to be able to recognize better the various phases. The thicknesses of the reaction zones were measured at four locations of the interface. The maximum thickness of the reaction zones was used to evaluate the kinetic data. In addition, some Scanning Electron Microscopy (SEM)/Energy Dispersive X-Ray (EDX) or SEM/Wave Length Dispersive X-Ray (WDX) examinations were performed to obtain information on the chemical compositions of the reaction products and diffusion zones.

The Zry crucibles from the pre-oxidized Zircaloy/Inconel interaction experiments, were oxidized in an Ar/O_2 mixture in a tube furnace. The selected temperature was 1000°C and the times needed to produce the oxide layer thicknesses of 20 and 45 µm were 6 and 25 minutes, respectively. Metallographic examinations were done to check the actual ZrO_2 layer thicknesses.

3. Results

The chemical interaction between Zircaloy and Inconel is a diffusion controlled process and can therefore be described quantitatively by Arrhenius equations. Besides the identification of the reacting species, phases, and the temperature of onset of liquid phase formation, one of the main results was the determination of the reaction kinetics, which may be used in a code system to predict the material behavior at high temperatures.

3.1 Chemical behavior

The chemical interaction between Inconel 718 (chemical composition of about 53

wt. % Ni, 19 % Cr, 18 % Fe, 6 % Nb+Ti, 3 % Mo) and Zircaloy-4 shows that a liquid reaction zone develops at temperatures as low as 1000°C. The melting points of Inconel 718 and Zircaloy-4 are 1335°C and 1760°C, respectively [3, 4].

Although many elements are involved in the Zry/Inconel chemical interaction, the binary phase diagrams offer a reasonable explanation of low temperature liquid phase formation. The (Ni - Zr), (Fe - Zr) and (Cr - Zr) phase diagrams indicate that eutectic interactions occur in these binary systems (Figures 2, 3) [5, 6]. The (Ni - Zr) system has four eutectic temperatures, with the lowest eutectic point at about 960°C on the Zr-rich side. The diffusion of approximately 2 wt. % Ni into β-Zr results in the formation of a liquid phase; even at this low temperature (Fig. 2) the eutectic temperature on the Ni side is about 1170°C. The lowest eutectic temperature exists in the (Fe - Zr) system at about 930°C also on the Zr-rich side, while the eutectic temperatures in the binary (Cr-Zr) system are 1332 and 1592°C, i.e. much higher.

The cross-sections of the Zry/Inconel reaction specimens after annealing at 1000, 1100, 1150 and 1200°C for various reaction times are shown in Figure 4. The cross-sections of both as-received and pre-oxidized Zry/Inconel reaction specimens (initial ZrO_2 layer thickness: 10 μm) are presented for comparison. The eutectic interactions, which occur at 1000°C and higher, result in the formation of liquid reaction products and voids form as some of the molten material relocates.

Although the specimens were annealed in an upright position, the reaction zones of the as-received Zry are not symmetrical around the circumference. Apparently, very small forces are sufficient to induce asymmetric reaction zones in the Zry wall. First interactions have been noticed at 1000°C after annealing times longer than 5 minutes. In all cases, the reaction in the Zry was much stronger than in Inconel. This may be explained by phase diagram considerations (Fig. 2, 3). Only small amounts ($\geq$ 5 wt. %) of Ni, Fe or Cr are necessary to liquefy large quantities of Zr. Also, since the eutectic temperatures in the (Ni - Zr), (Fe - Zr), and (Cr - Zr) systems are lowest on the Zr-rich side, Zr can be liquefied at much lower temperatures than Ni, Fe, or Cr. Liquefaction starts as soon as the liquidus line of the two phase field has been reached.

The cross sections of Zry-4/Inconel 718 specimens and typical microstructures produced by the chemical interactions are shown in Figures 5 through 10.

The solidified reaction zones were examined with SEM/EDX. Besides the determination of the element distribution, quantitative measurements were

performed. A typical result of a specimen annealed at 1150°C for 1 minute is shown in Figure 11. As can be recognized, the molten reaction zone consists of two layers formed due to the eutectic reaction, the morphology of the reaction zone was observed in the whole range of temperature and time examined. The element distribution shows Cr enrichment and Ni depletion in the thinner reaction layer I adjacent to the Inconel. In the reaction layer II, Zr, Ni and Fe are uniformely distributed, Cr is connected with precipitates in this zone.

The integral chemical analysis of the solidified melt of reaction layer I shows the following chemical composition: about 56 wt. % Zr, 23 % Cr, 9 % Fe, 5 % Ni, 5 % Mo, 2 % Nb. The integral analysis for the reaction layer II reveals: 82 wt. % Zr, 12 % Ni, 3 % Fe, 2 % Cr, 1 % Sn, which is very similar to the chemical composition of the eutectic point on the Zr-rich side in the (Ni - Zr) system (Fig. 2). From the binary (Ni - Zr) and (Fe - Zr) phase diagrams and the chemical composition of the reaction zone it is clear that the diffusion of Ni and Fe into Zry is initially responsible for the low-temperature liquefaction of Zircaloy. The further liquefaction of Zry may then occur faster by dissolution of the Zr in the liquid reaction product.

The metallic (Zr, Ni, Fe, Cr) melts in the two reaction layers decompose into various phases on cooldown. In Table 1 the results are entered of the quantitative analysis of the phases in the reaction zone.

A relation between the microstructure observed in the reaction zone and the ternary (Zr - Ni - Fe) and (Zr - Cr - Fe) phase diagrams at 1000°C [7] is shown in Figure 12. The integral chemical composition of the reaction zone (dark areas in the phase diagrams) lie in the liquid region for the reaction layer II and in the liquid/solid region for the reaction layer I. The chemical analysis is in agreement with the microstructure observed in the reaction layers.

During the isothermal interaction the liquid phase formed due to the (Ni - Zr) and (Fe - Zr) eutectic interactions penetrates along the grain boundaries of the Zr $(Cr, Fe)_2$ phase, which develops in the reaction layer I (Cr enriched zone) due to the diffusion of Zr into Inconel. This liquid/solid interaction dissolves to a certain extent the Zr $(Cr, Fe)_2$ phase; the amount and size of this phase decrease with increasing distance from the Inconel/liquid interface. In the reaction layer II, which is liquid at the reaction temperature, the Zr $(Cr, Fe)_2$ phase is present only in a very limited amount (Fig. 12). During cooldown the liquid alloy of reaction layers I and II starts to solidify and decomposes into the β-Zr and Zr_2 (Ni, Fe)

phases. The Cr_2 (Zr, Fe) phase was observed only in the reaction layer I at temperatures above 1150°C (Fig. 11).

3.2 Reaction kinetics

The behavior of the solid/solid contact interface of Zircaloy/Inconel in the temperature range 1000 - 1200°C shows the pronounced damage of Zircaloy, which is indicated by the extended thickness of the liquid reaction zone resulting from the chemical interactions. To be able to determine the reaction kinetics between Zry-4 and Inconel 718, the thicknesses of the reaction zones were measured as a function of the reaction time. The isothermal growth of the reaction zone (dissolution of Zry and Inconel) is a linear function of the square root of time (parabolic rate law) for all temperatures examined, indicating a diffusion-controlled process. The maximum thicknesses of the reaction zones in the Zry crucibles and Inconel rods in the as-received conditions are listed in Table2. The squares of the reaction zone thicknesses in Zry and Inconel are plotted as a function of the annealing times in Figure 13.

Ni and Fe diffuse into solid Zry and initiate Zry liquefaction as soon as the solid/liquid phase field has been reached. To show the differences in the amount of dissolved Zry and Inconel, the thicknesses of the reaction zones in Zry and Inconel are plotted in Figure 14 as a function of temperature for an annealing time of 5 minutes. Small amounts of Inconel dissolve large amounts of Zry. Above about 1250°C complete liquefaction of the specimens occurs.

The reaction zone growth rates for the Zry/Inconel interactions are listed in Table 3 and plotted as a function of the reciprocal temperature in Figure 15. The experimental data have been fitted by the following equation.

$$x^2/t = A \cdot \exp\ (-B/RT)$$

where

x (cm): reaction layer thickness, t (s): annealing time, A: pre-exponential factor, B (J/mol): activation energy, T (K): annealing temperature, R (J/mol·K): 8.314 gas constant

The growth rate equations determined for the temperature range of 1000 to 1200°C are:

for Zircaloy-4

$$x^2/t\ (cm^2/s) = 4.435 \cdot 10^4 \cdot \exp(-252093/RT)$$

for Inconel 718

$$x^2/t\ (cm^2/s) = 2.884 \cdot 10^5 \cdot \exp(-294962/RT)$$

These equations can be extrapolated to lower temperatures, but not to higher temperatures since fast and complete liquefaction of the materials takes place at about 1250°C.

3.3 Influence of an oxide layer on Zircaloy/Inconel interaction

The chemical interaction between pre-oxidized Zircaloy-4 and Inconel 718 (initial ZrO_2 layer thicknesses: 20 and 45 µm) indicate that the oxide layer delays the beginning of the interaction and reduces the reaction rate, but cannot prevent interaction. The cross section of Zry/Inconel reaction specimens annealed at 1000, 1100, 1150 and 1200°C for various reaction times are shown in Figure 4. The cross section of both as-received and pre-oxidized specimens (initial ZrO_2 layer thickness 10 µm) are presented for comparison. Inconel does not interact with stoichiometric ZrO_2, but the oxide layer will be dissolved by Zry, while forming oxygen-stabilized α-Zr(O) during a time-dependent incubation period, t_0. The delay in interaction (liquid phase formation) is determined by the time which is necessary for the oxygen to diffuse from the ZrO_2 layer into Zry forming a "metallic" oxygen-stabilized α-Zry(O) phase which can then interact with Inconel.

The experimental results with the pre-oxidized Zry specimens have shown that the liquefaction of the specimens has shifted to higher temperatures. The chemical reaction rate was slower when compared with the specimens tested in the as-received condition. Figures 16 and 17 show the cross sections of pre-oxidized Zry/Inconel specimens and a detail of the reaction zone produced by the chemical interaction at 1000 and 1200°C. The extent of the reaction in the as-received Zry condition is presented for comparison. It is clear, that the protective character of the ZrO_2 layer on the Zry surface, which acts initially as a barrier for the Zry/Inconel interactions, depends on the temperature, initial oxide layer

thickness and time. Figures 18 and 19 show the cross sections and typical microstructures produced by the chemical interaction between pre-oxidized Zry and Inconel as a function of time. Liquid phase formation starts before the oxide layer has completely disappeared. Figures 17 and 19 show that a thin porous oxide layer remains in the liquid reaction zone; the same effect was seen in the chemical interaction between Zry-4 and 1.4919ss (AISI 316) [8]. The oxygen from the ZrO_2 layer diffuses into Zry, stabilizing the α-Zry(O) phase, and forms a sub-stoichiometric ZrO_{2-x} oxide layer. In this way, Zr from the oxide layer can interact with Ni and Fe, producing a liquid phase on the Inconel side which penetrates through the cracks of the brittle oxide layer reaching the α-Zry (O) phase.

The thicknesses of the reaction zones in Zry and Inconel measured for the pre-oxidized Zry/Inconel reaction specimens are listed in Tables 4 and 5 for an initial ZrO_2 thickness of 20 and 45 μm, respectively.The square of the reaction thicknesses versus the annealing times are plotted in Figures 20 and 21. The differences in the thicknesses of the liquid reaction zones between Zry and Inconel are smaller at 1200°C and above than at lower temperatures; the same has been found in the experiments performed with specimens in the as-received condition. The reason is that at the temperature of about 1170°C eutectic interaction develops between Ni and Zr on the Ni-rich side (phase diagram in Fig. 2); only small amounts of Zr (< 3 wt. %) are necessary to produce a liquid phase at this temperature by diffusion processes.

The calculated isothermal growth rates are listed in Tables 6 and 7 for the initial ZrO_2 thicknesses of 20 and 45 μm, respectively, and plotted versus the reciprocal temperature in Figures 22 and 23. The growth rate equations and 't_0' values have been determined from the x^2 versus t correlation of the experimental data. In Figures 24 and 25 a comparison is made of the growth rates of Zry and Inconel, respectively, as a function of the reciprocal temperature for the different conditions of the Zry/Inconel reaction couple. The results indicate that a ZrO_2 layer delays the chemical interaction between Zry and Inconel. However, the protective effect of the oxide layer could be inhibited at the contact point of both materials if the interaction took place in an oxidizing atmosphere. To clarify this point, a few experiments were done in steam atmosphere using the configuration schematically represented in Figure 26. The interaction was demonstrated by several molten zones on the external surface of the Zry tube in the regions of contact. A cross section of a sample heated at 1150°C for 3 min. is

shown in Figure 27. Liquid phase formation due to the chemical interactions is not prevented under conditions of unlimited steam oxidation.

4. Discussion

The main purpose of this work has been to determine the kinetics of reaction between Zircaloy and Inconel with a view of understanding and describing analytically the chemical interactions between the Zircaloy-4 fuel rod cladding tubes and Inconel 718 spacer grids in integral experiments like the CORA tests [9]. Although some interaction experiments have been described in the literature [10, 11], no Arrhenius equation had been previously been developed from the data. In all cases, the maximum thickness of the reaction zone was used in the evaluation of the kinetic data to obtain conservative results.

In the Zry/Inconel system, a considerable amount of liquid phase is formed around 1000°C; the amount of liquefied material increases with increasing temperature and time. The nickel-zirconium and iron-zirconium phase diagrams (Figs. 2, 3) show that due to eutectic interactions early melt generation has to be expected which initiates melt progression within the fuel assembly at low temperatures.

The results of the present single-effect tests are in agreement with results of integral tests (CORA experiments) where fuel rod bundles were heated to temperatures of about 2000°C [9]. In all cases, damage to the bundle was initiated by Zircaloy/Inconel and Zircaloy/stainless steel interactions. Localized liquefaction of these components started at around 1200°C. The low-temperature melt formation initiates bundle damage and causes the chemical attack of the fuel rods dissolving the Zry cladding tubes and part of the UO_2 fuel. By this process, molten fuel formation and relocation as well as early fission product release can take place even well below the melting point of Zry. The melts relocate towards cooler regions of the core where they may cause coolant channel blockages upon solidification.

Thin oxide layers on the Zry surface can delay the chemical interactions with Inconel, but cannot prevent them. ZrO_2 interacts with metallic Zr while forming oxygen-stabilized α-Zr(O) resulting in a sub-stoichiometric ZrO_2. α-Zr (O) is capable of interacting with the Inconel alloy components. The oxygen dissolved in the Zry lattice exerts an influence on the diffusion and/or dissolution processes; the reaction rates are slower. In all other cases, the reaction of Zry with oxygen or steam is more favorable thermodynamically than the reactions with

Inconel, but as the integral bundle meltdown experiments [9] show, a steam environment cannot prevent the chemical interaction between Zry and Inconel.

The chemical analysis of the reaction zone in the single-effect tests showed a great similarity in the chemical composition of some phases (developed during the chemical interactions) compared with the analysis of integral CORA experiments [9] and chemical analysis on selected samples from the TMI-2 reactor core [7], for example the phases Zr_2 (Ni, Fe) and β-Zr.

The chemical interactions which take place during the integral fuel bundle tests could be explained only by the single-effects test results. The complexity of a severe reactor accident scenario with the resulting multitude of materials interactions make a complete interpretation of the many possible chemical interactions extremely difficult and in some cases even impossible.

5. Summary and Conclusions

- Inconel 718 in contact with Zircaloy gives rise to chemical interactions which can be described by a parabolic rate law.
- As a result of eutectic interactions at temperatures as low as 1000°C, the liquid phase causes a fast and complete liquefaction of both components of the reaction couple at about 1250°C.
- Only a small amount of Inconel is necessary to liquefy large amounts of Zry.
- Thin ZrO_2 layers on the Zircaloy surface delay liquid phase formation and reduce the rates of reaction, but cannot prevent the chemical interaction.
- In experiments of short durations, the ZrO_2 layers shift the liquefaction temperature to higher values; the required incubation period depends on the initial oxide layer thickness and on the temperature.
- Liquid phase formation due to the chemical interactions at low temperatures is not prevented under unlimited steam oxidation conditions.

6. Acknowledgement

The authors wish to thank Dr. T. Haste (AEA Technology, Winfrith) for his thorough and critical review of this paper.

This work was partially funded by the Commission of the European Communities under the Reinforced Concerted Action Project "Core Degradation", Contract Number FI3S-CT92-0001.

7. References

[1] S. Hagen, P. Hofmann, G. Schanz, L. Sepold; Interaction in Zircaloy/UO_2 Fuel Rod Bundles with Inconel Spacer at Temperatures above 1200°C; Results of the Experiments CORA-2 and CORA-3, KfK Report 4378,1990.

[2] P. Hofmann et al.; Low-Temperature Liquefaction of LWR Core Components, Severe Accident Research Program Review Meeting, Brookhaven National Laboratory, Upton, New York, April 30 - May 4, 1990.

[3] Metals handbook, Vol. 1, 10th edition, 1990, ASM International, Materials Park, OH, USA.

[4] G. Miller; Zirconium; Academic Press Inc., Publishers 111, N. Y., 1986

[5] T. B. Massalski; Binary alloy phase diagrams, Vols. 1, 2, American Society for Metals, Ohio, 1986.

[6] D. Arias, J. P. Abriata; The Fe-Zr system, Bulletin of Alloy Phase Diagrams, Vol. 9, No. 5, 597 - 604,1988.

[7] H. Kleykamp, R. Pejsa; Chemical and X-Ray Diffraction Analysis on Selected Samples from the TMI-2 Reactor Core, KfK 4872; May 1991.

[8] P. Hofmann, M. Markiewicz; Chemical interaction between as-received and pre-oxidized Zircaloy-4 and stainless steel at high temperatures; KfK 5106,1994.

[9] S. Hagen, P. Hofmann, G. Schanz, L. Sepold; Results of the severe CORA fuel damage experiments CORA-2 and CORA-3; KfK 4376, 1989.

[10] B. Daniel, A. Nichols, J. Simpson; The liquefaction of alloys identified with structural materials in a PWR core; AEEW-M 2250, Dec. 1985.

[11] F. Nagase, T. Otomo, H. Uetsuka; Interaction between Zircaloy tube and Inconel spacer grid at high temperature; JAERI-M 90 - 165, 1990.

List of Tables

Table 1: Quantitative analysis of phases in the Zircaloy-4/Inconel 718 reaction zone (Fig. 12).

Table 2: Measured total thicknesses of reaction zones in Zircaloy and Inconel for the as-received Zircaloy-4/Inconel 718 diffusion couple as a function of temperature and time (Fig. 13).

Table 3: Reaction zone growth rates in Zircaloy and Inconel for the as-received Zircaloy-4/Inconel 718 diffusion couple (Fig. 15).

Table 4: Measured total thicknesses of reaction zones in Zircaloy and Inconel for the pre-oxidized Zircaloy-4/Inconel 718 diffusion couple; initial ZrO_2 oxide layer thickness: 20 µm (Fig. 20).

Table 5: Measured total thicknesses of reaction zones in Zircaloy and Inconel for the pre-oxidized Zircaloy-4/Inconel 718 diffusion couple; initial ZrO_2 oxide layer thickness: 45 µm (Fig. 21).

Table 6: Reaction zone growth rates in Zircaloy and Inconel for the pre-oxidized Zircaloy-4/Inconel 718 diffusion couple; initial ZrO_2 oxide layer thickness: 20 µm (Fig. 22).

Table 7: Reaction zone growth rates in Zircaloy and Inconel for the pre-oxidized Zircaloy-4/Inconel 718 diffusion couple; initial ZrO_2 oxide layer thickness: 45 µm (Fig. 23).

List of Figures

Fig. 1: Setup of the reaction couples.

Fig. 2: Binary phase diagram of the Ni-Zr system [5].

Fig. 3: Binary phase diagrams of the Fe-Zr and Cr-Zr systems [5, 6].

Fig. 4: Chemical interactions between Zircaloy-4 and Inconel 718 at different temperatures; influence of a thin ZrO_2 layer on the reaction behavior (right column of pictures).

Fig. 5: Chemical interactions between Zircaloy-4 and Inconel 718; annealing conditions: 1000°C/5 min.

Fig. 6: Chemical interactions between Zircaloy-4 and Inconel 718; annealing conditions: 1000°C/15 min.

Fig. 7: Chemical interactions between Zircaloy-4 and Inconel 718; annealing conditions: 1100°C/ 2 min.

Fig. 8: Chemical interactions between Zircaloy-4 and Inconel 718; annealing conditions: 1100°C/10 min.

Fig. 9: Chemical interactions between Zircaloy-4 and Inconel 718; annealing conditions: 1150°C 1 min.

Fig. 10: Chemical interactions between Zircaloy-4 and Inconel 718; annealing conditions: 1150°C / 2 min.

Fig. 11: Chemical composition of the Zircaloy-4/Inconel 718 reaction zone after 1 min at 1150°C.

Fig. 12: Isothermal section of the Fe-Zr-Ni and Fe-Zr-Cr system at 1000°C [7]. Relation between the observed microstructures and the phase diagrams (Table 1).

Fig. 13: Maximum reaction zone thicknesses in Zircaloy and Inconel for the Zircaloy-4/Inconel 718 system between 1000 and 1200°C (Table 2).

Fig. 14: Comparison of the reaction zone thicknesses in Zircaloy and Inconel for the Zircaloy-4/Inconel 718 system versus temperature; annealing time: 5 min.

Fig. 15: Reaction zone growth rates for the Zircaloy-4/Inconel 718 reaction system (Table 3).

Fig. 16: Chemical interactions between Zircaloy-4 and Inconel 718; 1000°C/30 min. Influence of a 20 µm thick ZrO_2 layer.

Fig. 17: Chemical interactions between Zircaloy-4 and Inconel 718; 1200°C/5 min. Influence of ZrO_2 layers of different thicknesses.

Fig. 18: Chemical interactions between pre-oxidized Zircaloy-4 and Inconel 718 as a function of time.

Fig. 19: Chemical interactions between pre-oxidized Zircaloy-4 and Inconel 718 as a function of time.

Fig. 20: Maximum reaction zone thicknesses in Zircaloy and Inconel for the pre-oxidized Zircaloy-4/Inconel 718 systems; initial ZrO_2 layer thickness: 20 µm (Table 4).

Fig. 21: Maximum reaction zone thicknesses in Zircaloy and Inconel for the pre-oxidized Zircaloy-4/Inconel 718 system; initial ZrO_2 layer thickness: 45 µm (Table 5).

Fig. 22: Reaction zone growth rates for the pre-oxidized Zircaloy-4/Inconel 718 system; initial ZrO_2 layer thickness: 20 µm (Table 6).

Fig. 23: Reaction zone growth rates for the pre-oxidized Zircaloy-4/Inconel 718 system; initial ZrO_2 layer thickness: 45 µm (Table 7).

Fig. 24: Reaction zone growth rates in Zircaloy for the as-received and pre-oxidized Zircaloy-4/Inconel-718 system; influence of ZrO_2 layer thickness on reaction rate.

Fig. 25: Reaction zone growth rates in Inconel for the as-received and pre-oxidized Zircaloy-4/Inconel-718 system; influence of ZrO_2 layer thickness on reaction rate.

Fig. 26: Schematic of the Zircaloy-4 tube/Inconel 718 grid system spacer used in experiments under oxidizing conditions (steam).

Fig. 27: Chemical interactions between Zircaloy-4 tube and Inconel 718 after 3 min at 1150°C in steam atmosphere.

Table 1: Quantitative analysis of phases in the Zircaloy-4/ Inconel 718 reaction zone (Fig. 12).

Reaction layer (see Fig. 12)	Element	Conc. in at. %	Phase
I, II	Zr	95	β-Zry
	Sn	2	
	Ni, Fe, Cr	3	
I,II	Zr	68	$Zr_2 (Ni, Fe)_2$
	Ni	22	
	Fe	7	
	Cr	3	
I, II	Cr	48	$Zr (Cr, Fe)_2$
	Zr	34	
	Fe	11	
	Mo	4	
	Ni	3	
I	Cr	65	$Cr_2 (Zr, Fe)$
	Zr	12	
	Fe	11	
	Mo	7	
	Ni, Nb	5	

Table 2: Measured total thicknesses of reaction zones in Zircaloy and Inconel for the as-received Zircaloy-4/Inconel 718 diffusion couple as a function of temperature and time (Fig. 13).

Specimen	Temperature °C	Time min	Reaction zone thickness, µm	
			Zircaloy-4	Inconel 718
29	1000	30	675	230
30	"	60	790	255
28	"	120	1290	550
31	1100	10	720	200
32	"	15	975	275
36	1200	3	995	507
35	"	5	1315	700

Table 3: Reaction zone growth rates in Zircaloy and Inconel for the as-received Zircaloy-4/Inconel 718 diffusion couple(Fig. 15).

Temperature °C	Reaction zone growth rate, x^2/t cm^2/s	
	Zircaloy-4	Inconel 718
1000	$2.17 \cdot 10^{-6}$	$3.25 \cdot 10^{-7}$
1100	$9.40 \cdot 10^{-6}$	$7.74 \cdot 10^{-7}$
1200	$5.66 \cdot 10^{-5}$	$1.55 \cdot 10^{-5}$

Rate equations:

For Zircaloy-4

$$x^2/t\ (cm^2/s) = 4.435 \cdot 10^4 \cdot \exp(-252093/RT)$$

For Inconel 718

$$x^2/t\ (cm^2/s) = 2.884 \cdot 10^5 \cdot \exp(-294962/RT)$$

$R = 8.314\ J/mol \cdot K$

Table 4: Measured total thicknesses of reaction zones in Zircaloy and Inconel for the pre-oxidized Zircaloy-4/Inconel 718 diffusion couple; initial ZrO_2 oxide layer thickness: 20 µm (Fig. 20).

Specimen	Temperature	Time min	Reaction zone thickness, µm	
			Zircaloy-4	Inconel
009	1100	120	240	140
037	"	180	1890	514
011	1200	5	400	255
010	"	10	840	975
012	"	15	1440	
041	1300	1	740	856
049	"	1.5	1008	1130

Table 5: Measured total thicknesses of reaction zones in Zircaloy and Inconel for the pre-oxidized Zircaloy-4/Inconel 718 diffusion couple; initial ZrO_2 oxide layer thickness: 45 µm (Fig. 21).

Specimen	Temperature	Time min	Reaction zone thickness, µm	
			Zircaloy-4	Inconel
043	1100	180	290	110
044	"	300	1095	306
023	1200	5	190	105
022	"	10	595	485
024	"	15	850	930
047	1300	1	440	290
048	"	2	1040	1255

Table 6: Reaction zone growth rates in Zircaloy and Inconel for the pre-oxidized Zircaloy-4/Inconel 718 diffusion couple; initial ZrO_2 layer thickness: 20 µm (Fig. 22).

Temperature °C	Reaction zone growth rate, x^2/t cm^2/s	
	Zircaloy-4	Inconel 718
1100	$9.76 \cdot 10^{-6}$	$6.79 \cdot 10^{-7}$
1200	$3.18 \cdot 10^{-5}$	$2.95 \cdot 10^{-5}$
1300	$1.51 \cdot 10^{-4}$	$1.80 \cdot 10^{-4}$

Rate equations:

For Zircaloy-4

$$x^2/(t-t_0)\ (cm^2/s) = 20952 \cdot \exp(-246427/RT)$$

For Inconel 718

$$x^2/(t-t_0)\ (cm^2/s) = 1.727 \cdot 10^{13} \cdot \exp(-507395/RT)$$

$R = 8.314\ J/mol \cdot K$

t_0 values, s

°C	Zry-4	Inconel
1100	7175	6912
1200	314	339
1300	24	20

Table 7: Reaction zone growth rates in Zircaloy and Inconel for the pre-oxidized Zircaloy-4/Inconel 718 diffusion couple; initial ZrO_2 layer thickness: 45 µm (Fig. 23).

Temperature °C	Reaction zone growth rate, x^2/t cm^2/s	
	Zircaloy-4	Inconel 718
1100	$1.55 \cdot 10^{-6}$	$1.12 \cdot 10^{-7}$
1200	$1.14 \cdot 10^{-5}$	$1.42 \cdot 10^{-5}$
1300	$1.48 \cdot 10^{-4}$	$2.49 \cdot 10^{-4}$

Rate equations:

For Zircaloy-4

$$x^2/(t-t_0)\ (cm^2/s) = 5.44 \cdot 10^9 \cdot \exp(-410306/RT)$$

For Inconel 718

$$x^2/(t-t_0)\ (cm^2/s) = 5.4 \cdot 10^{19} \cdot \exp(-699018/RT)$$

$R = 8.314\ J/mol \cdot K$

t_0 values, s

°C	Zry-4	Inconel
1100	12900	9741
1200	276	340
1300	68	40

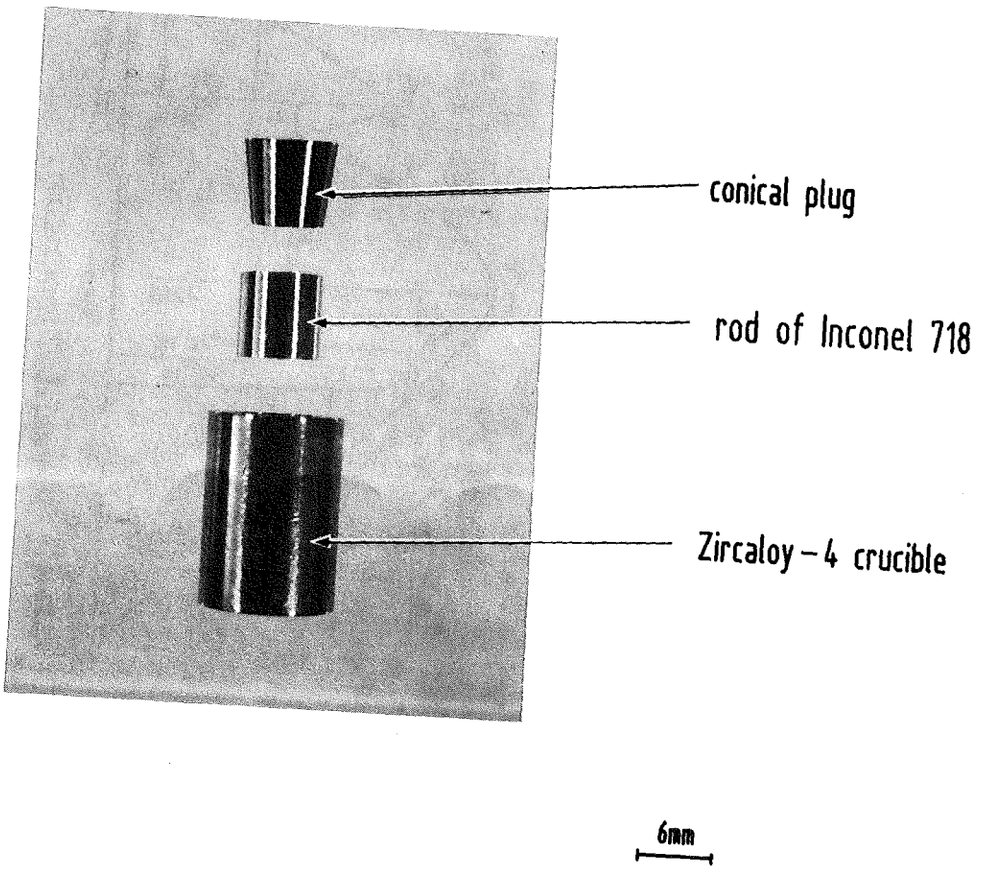

Fig. 1: Setup of the reaction couples.

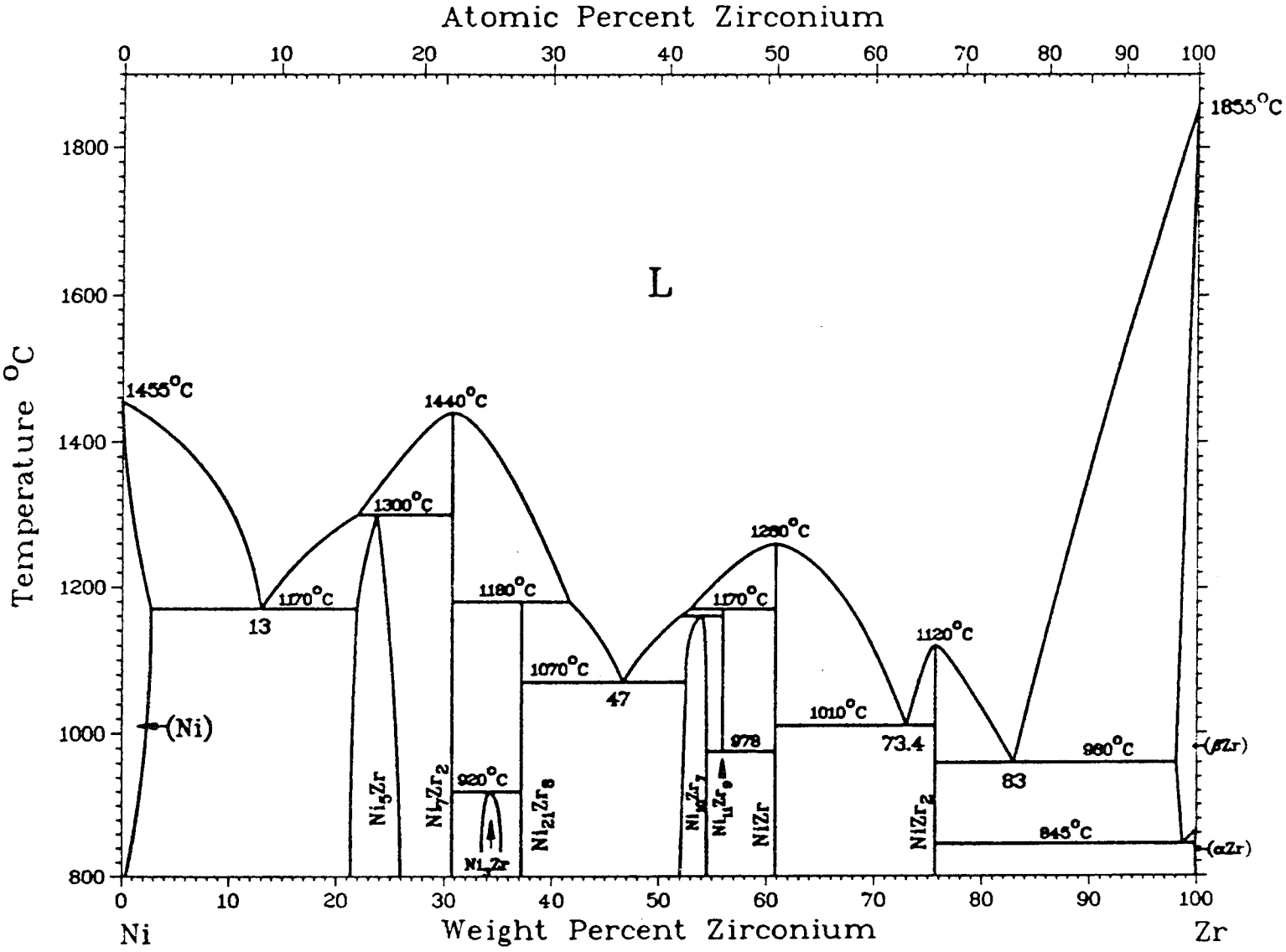

Fig. 2: Binary phase diagram of the Ni-Zr system [5].

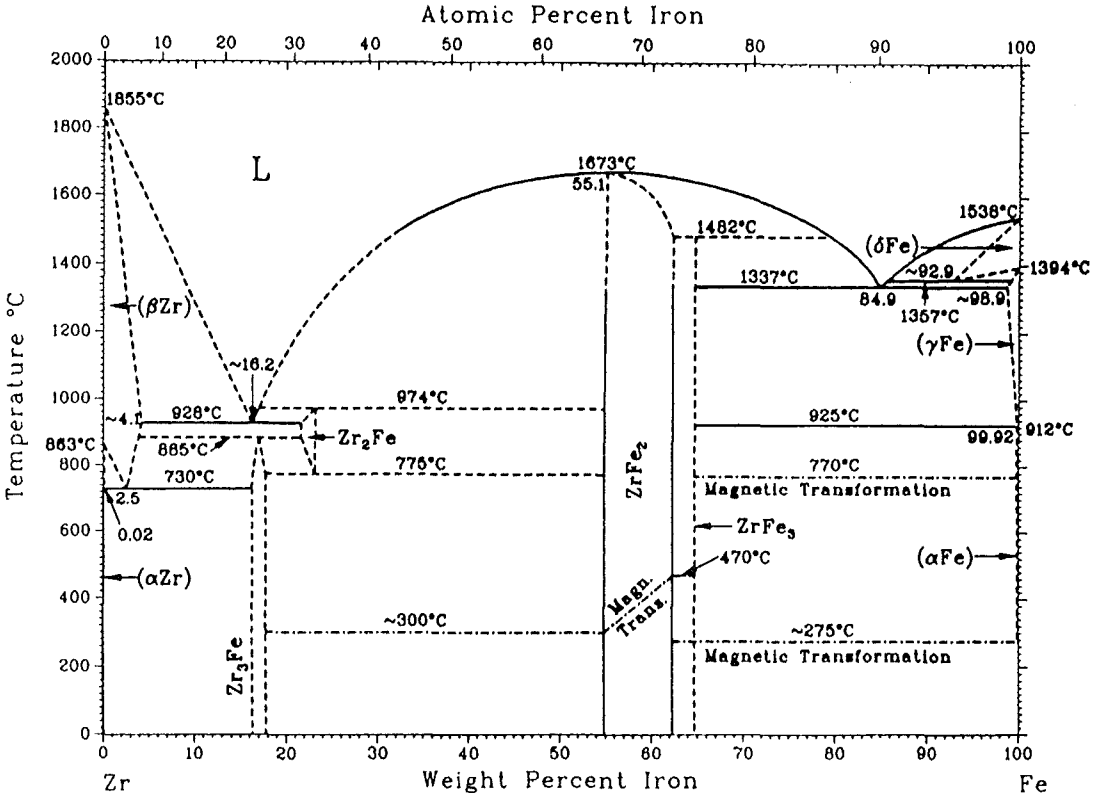

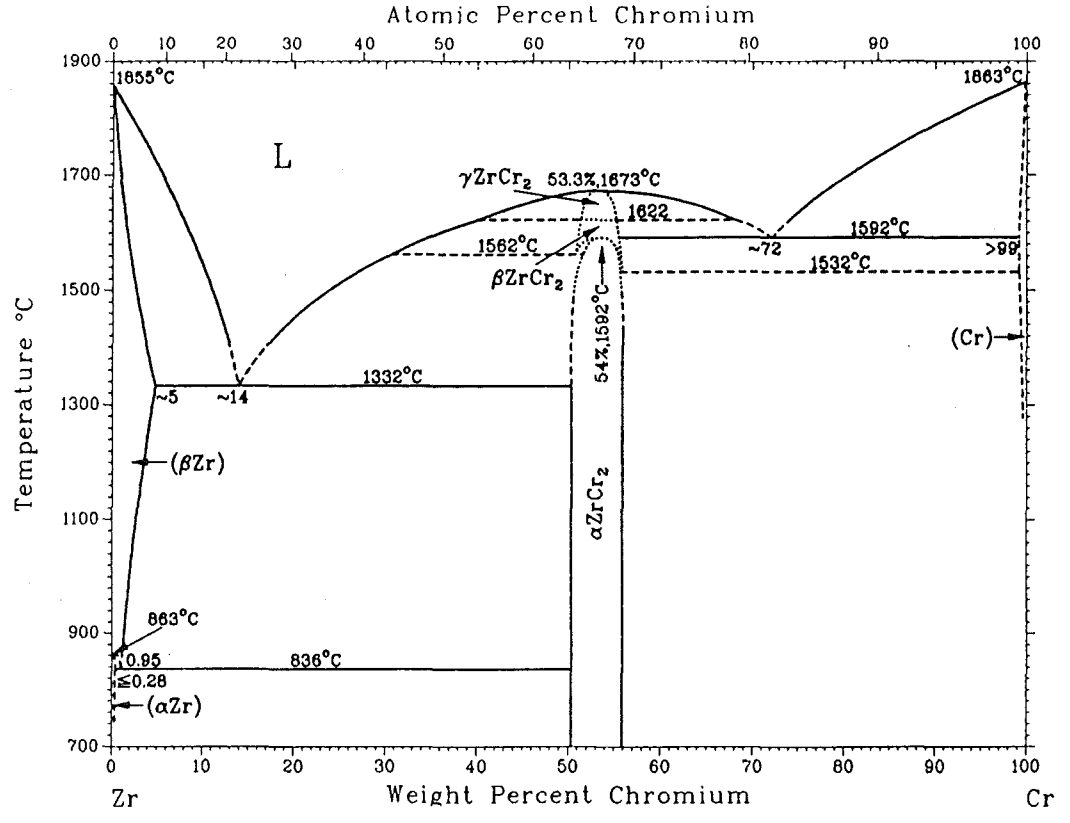

Fig. 3: Binary phase diagrams of the Fe-Zr and Cr-Zr systems [5, 6].

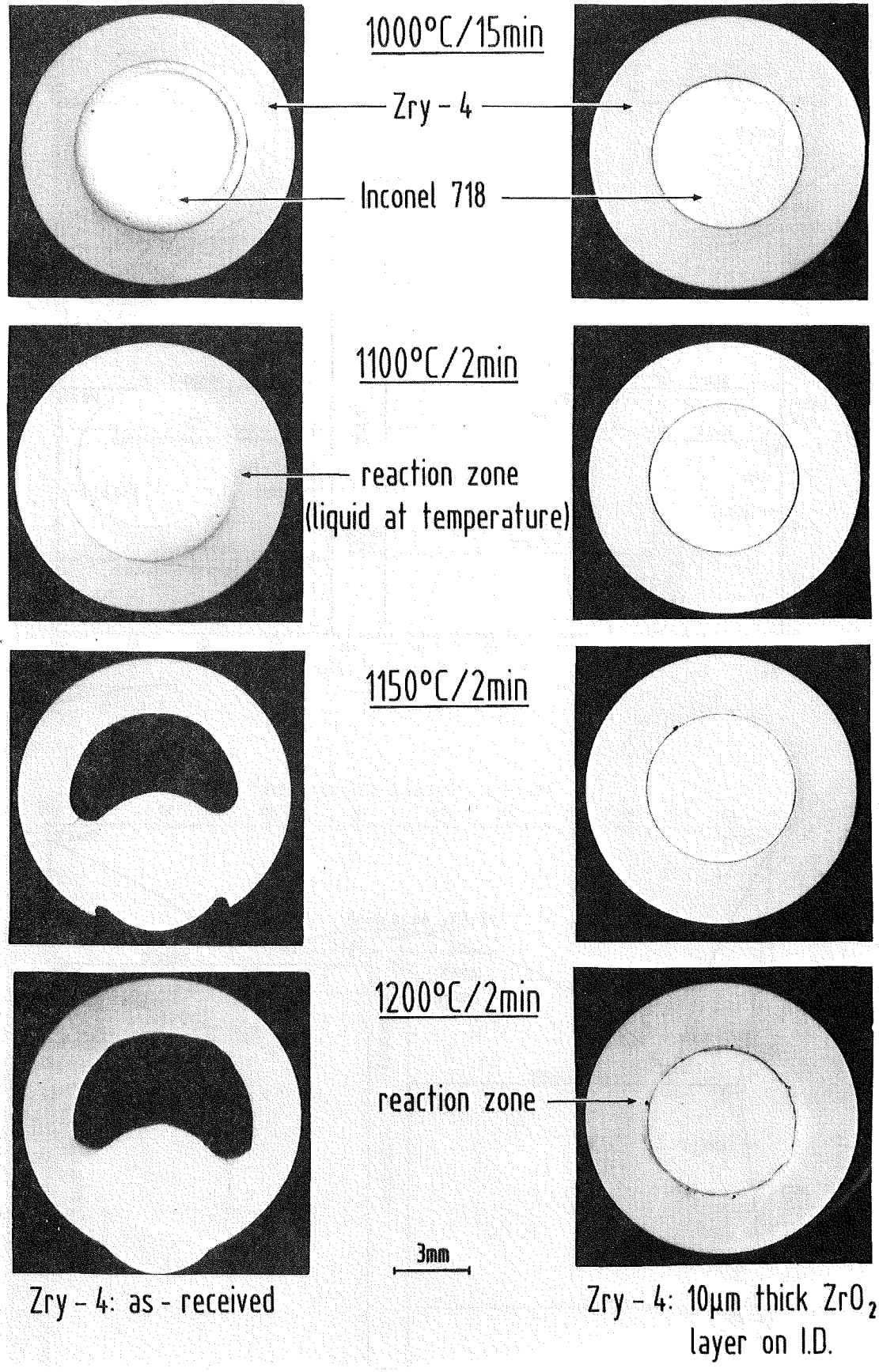

Fig. 4: Chemical interactions between Zircaloy-4 and Inconel 718 at different temperatures; influence of a thin ZrO_2 layer on the reaction behavior (right column of pictures).

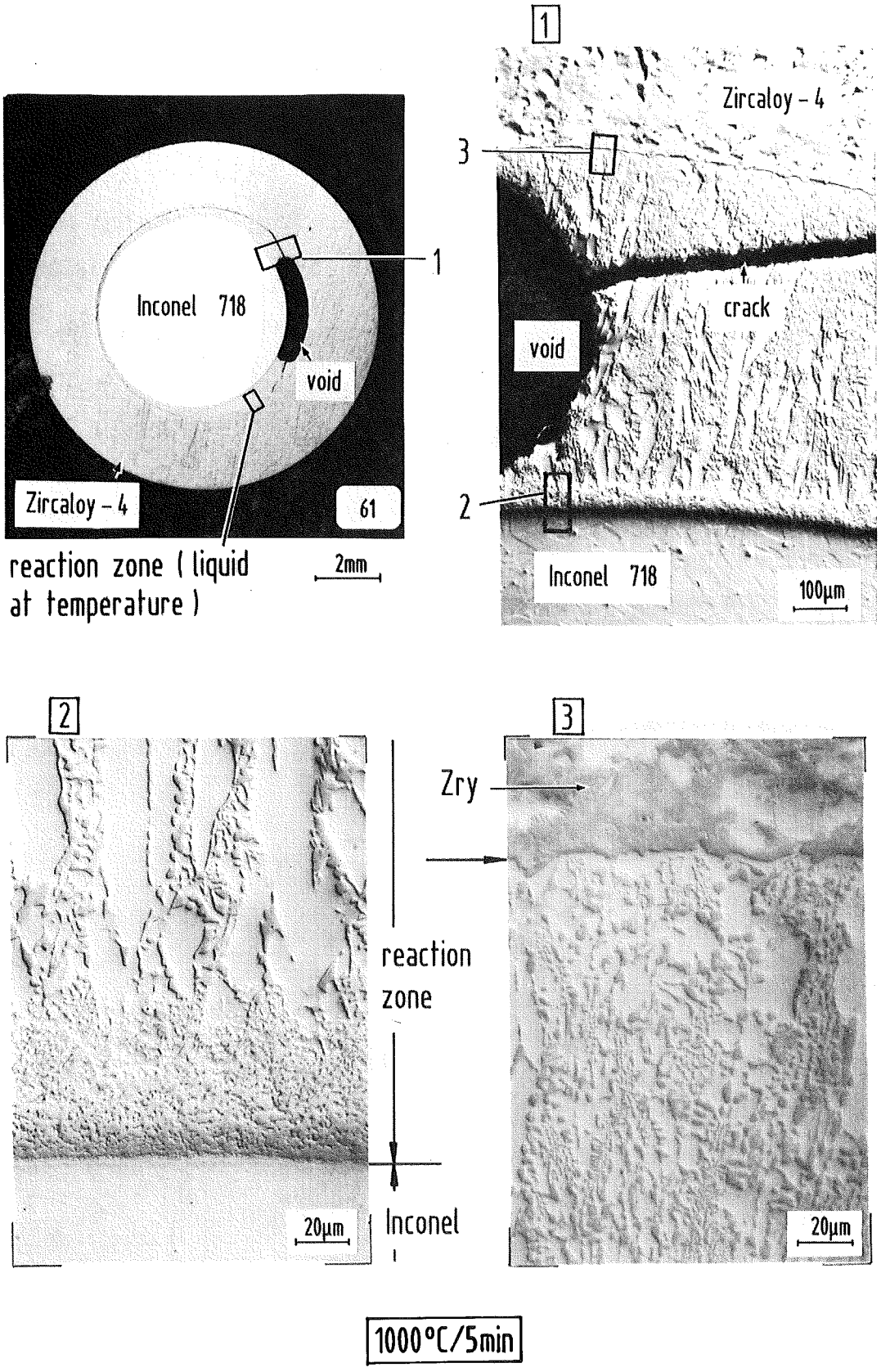

Fig. 5: Chemical interactions between Zircaloy-4 and Inconel 718; annealing conditions: 1000°C/5 min.

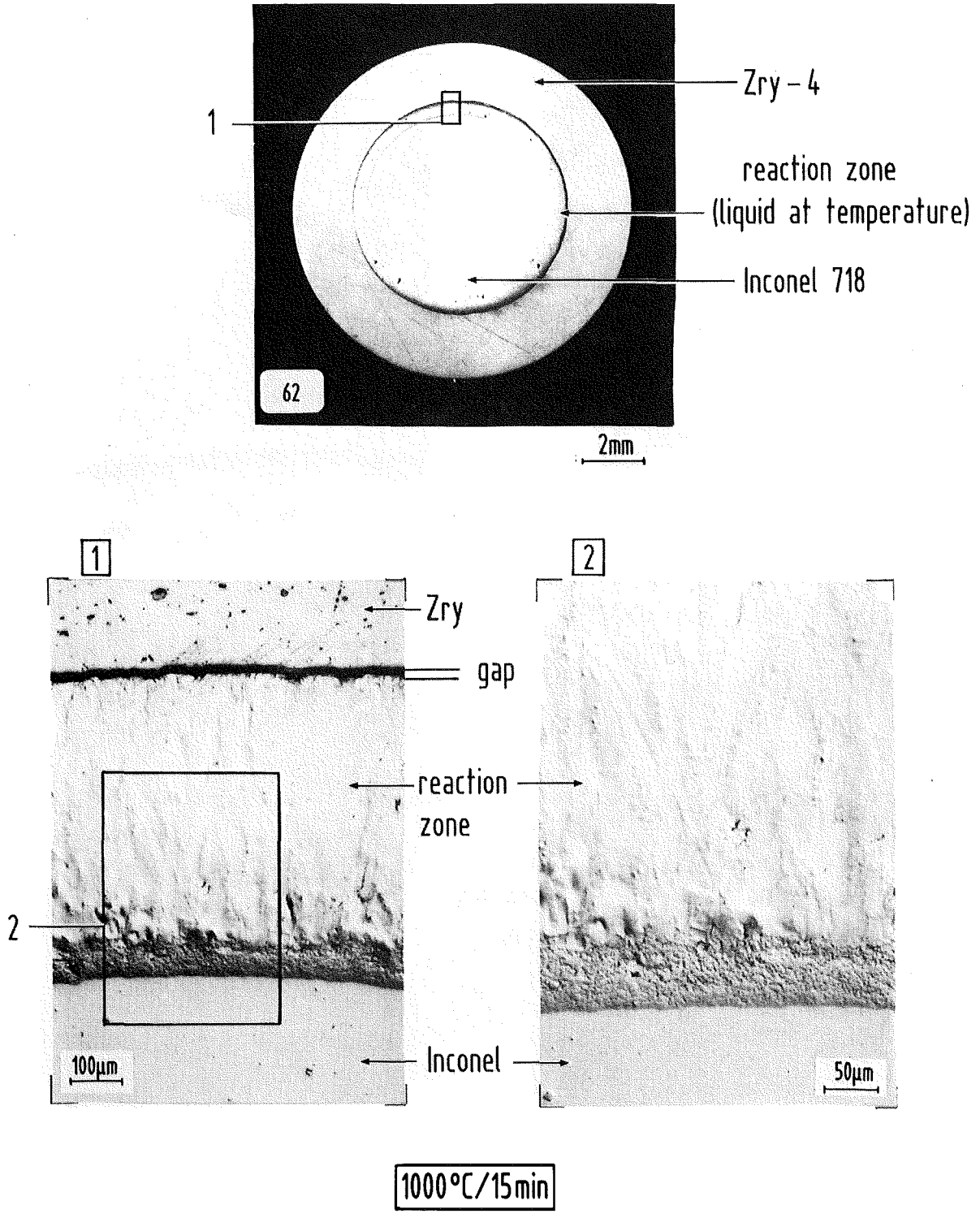

Fig. 6: Chemical interactions between Zircaloy-4 and Inconel 718; annealing conditions: 1000°C/15 min.

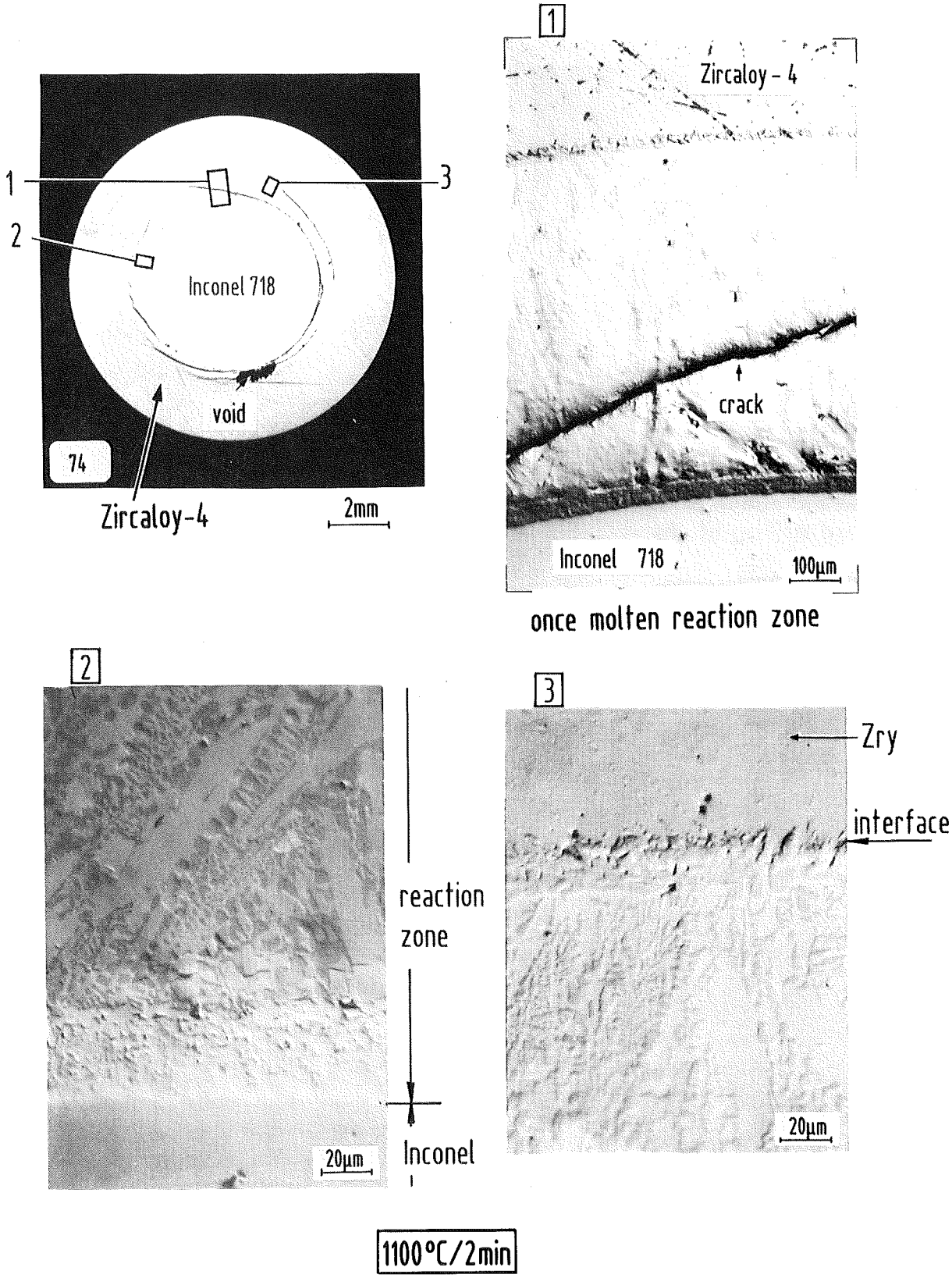

Fig. 7: Chemical interactions between Zircaloy-4 and Inconel 718; annealing conditions: 1100°C/ 2 min.

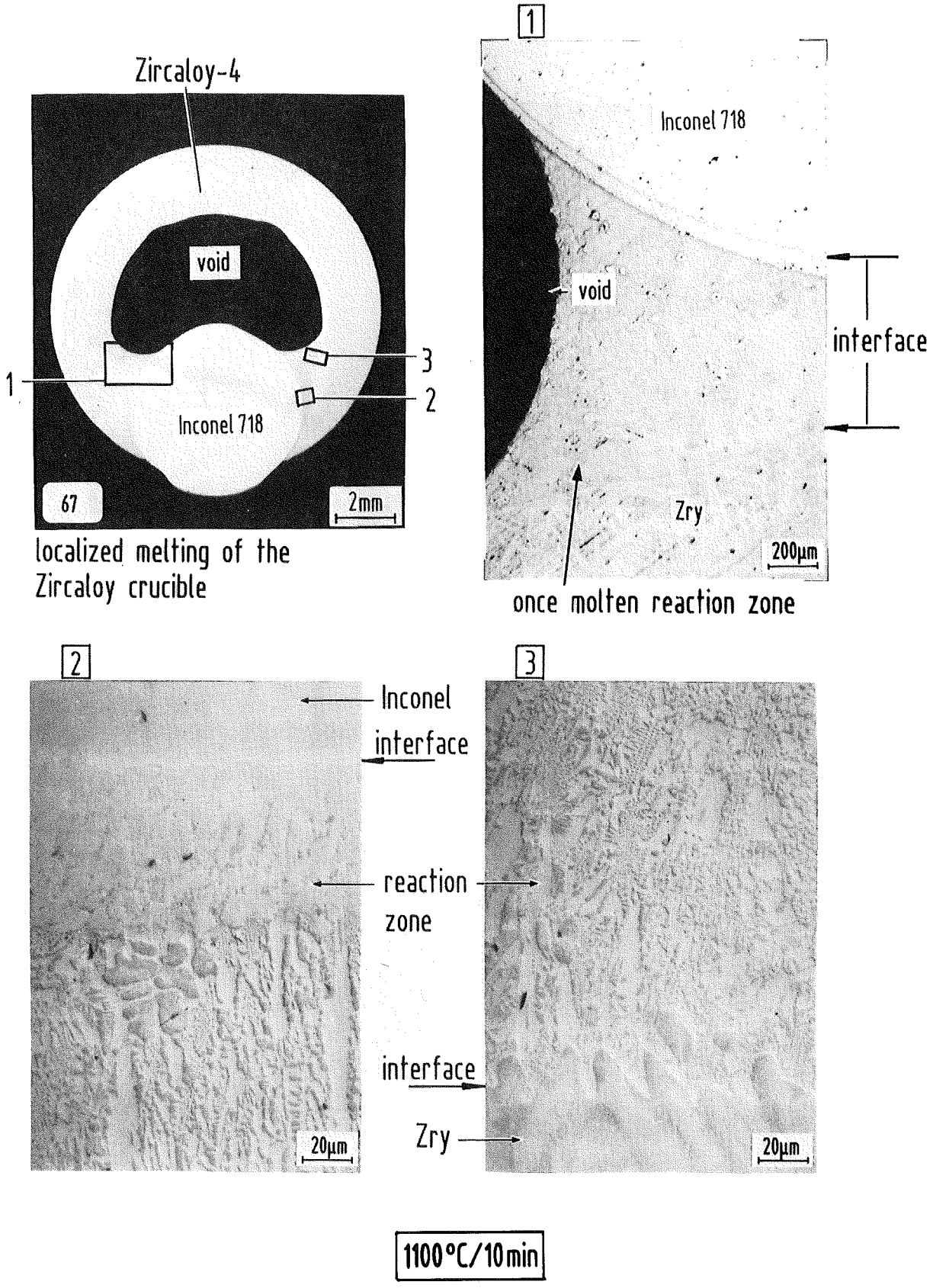

Fig. 8: Chemical interactions between Zircaloy-4 and Inconel 718; annealing conditions: 1100°C/10 min.

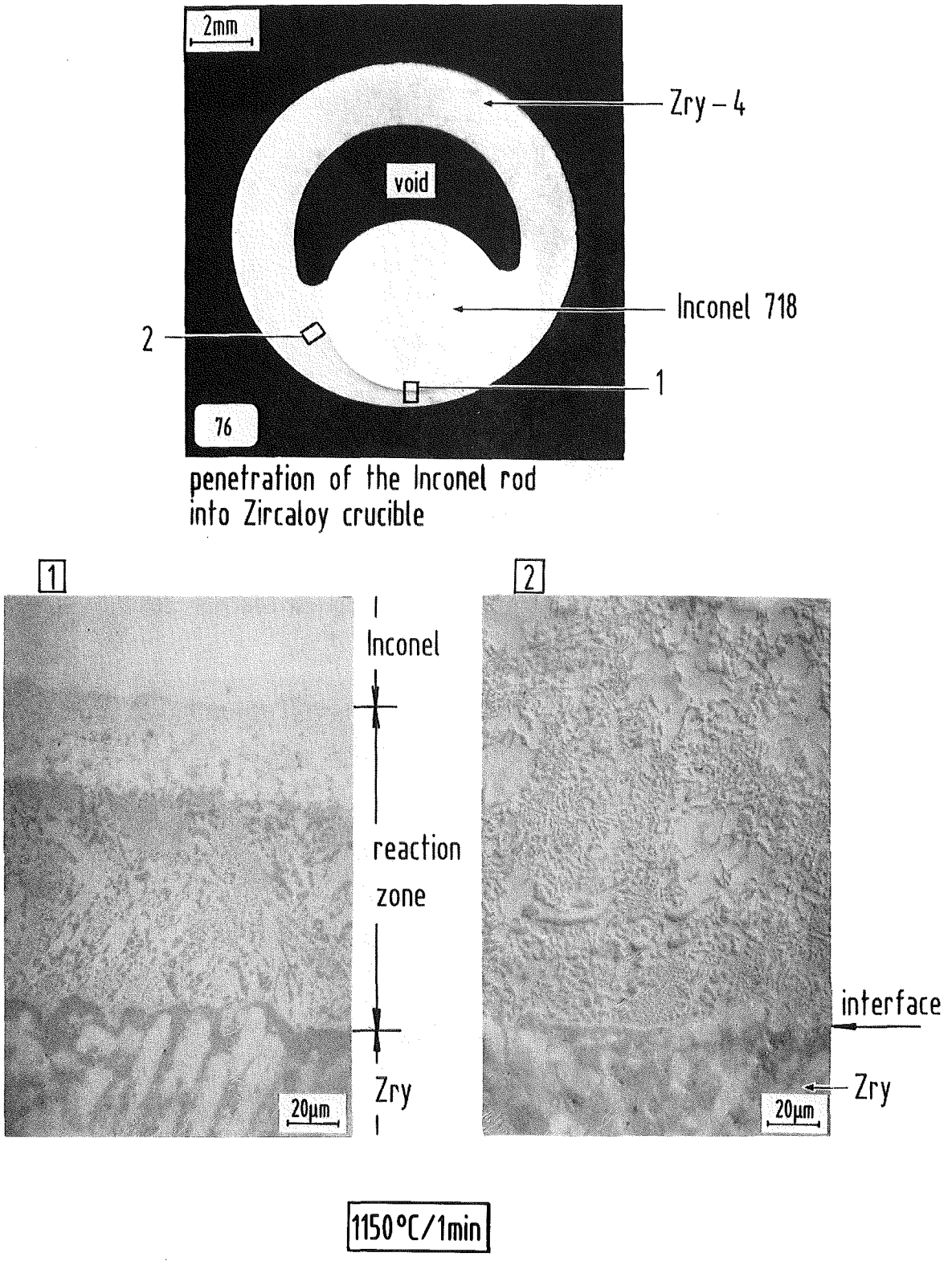

Fig. 9: Chemical interactions between Zircaloy-4 and Inconel 718; annealing conditions: 1150°C 1 min.

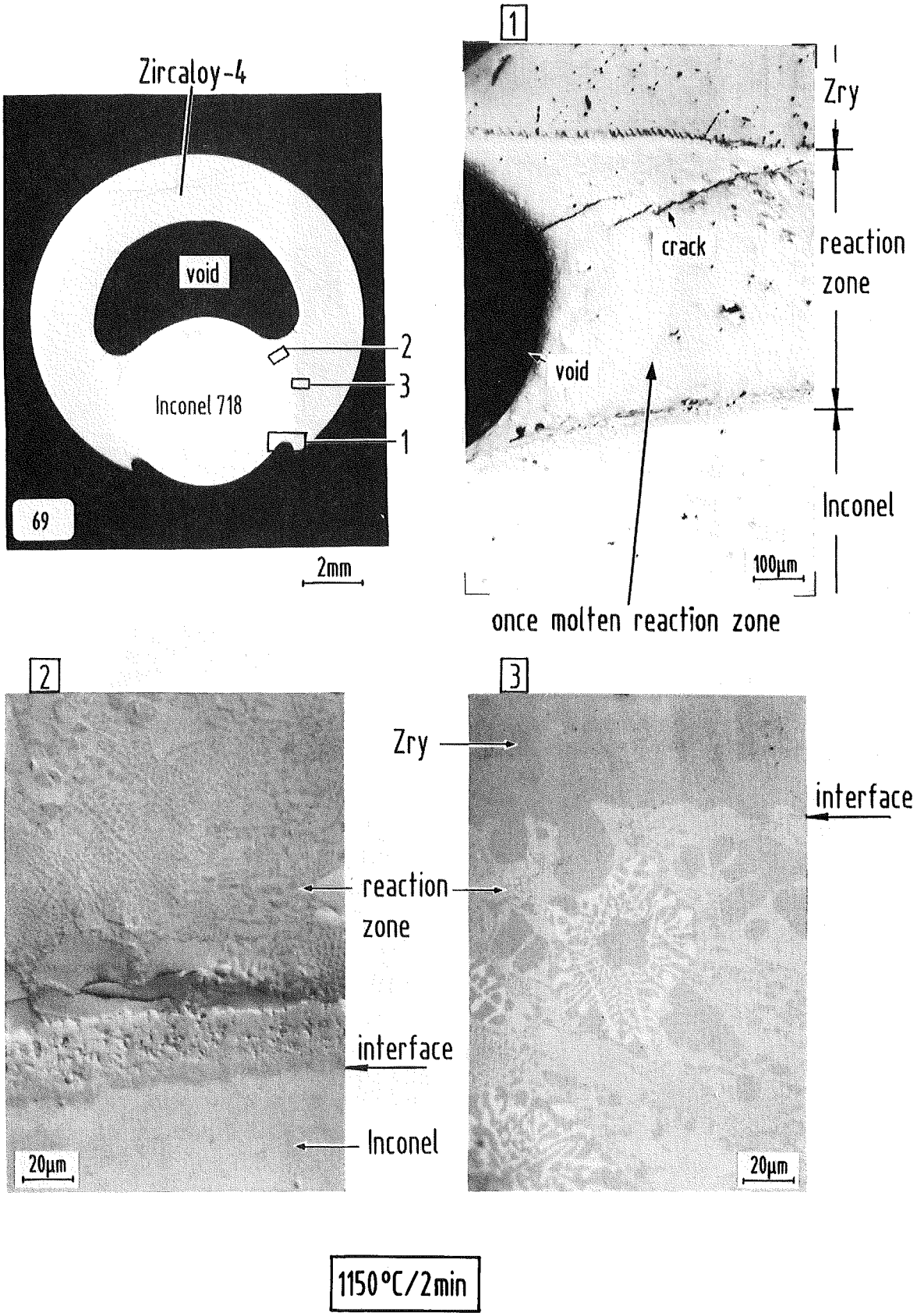

Fig. 10: Chemical interactions between Zircaloy-4 and Inconel 718; annealing conditions: 1150°C / 2 min.

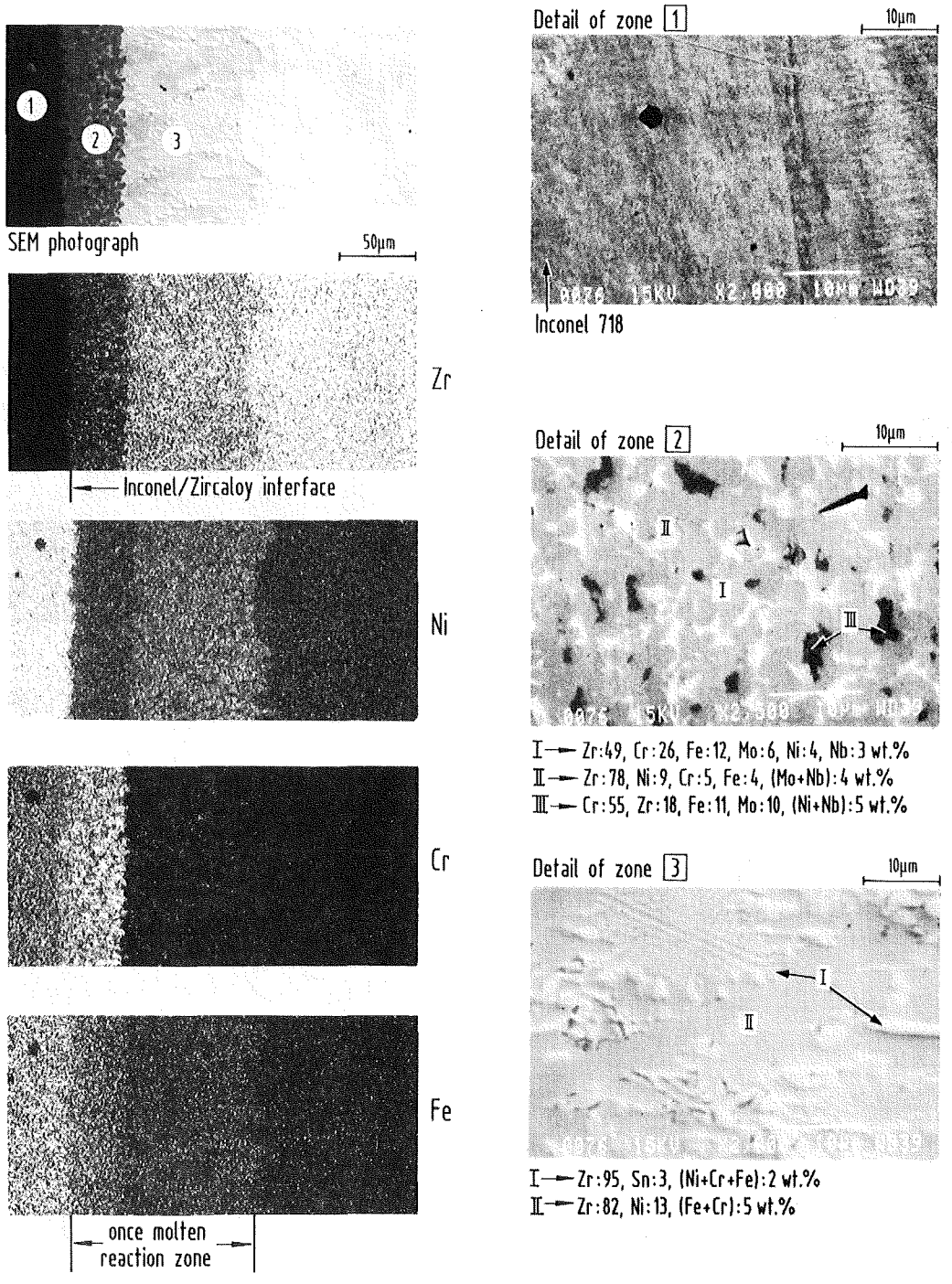

Fig. 11: Chemical composition of the Zircaloy-4/Inconel 718 reaction zone after 1 min at 1150°C.

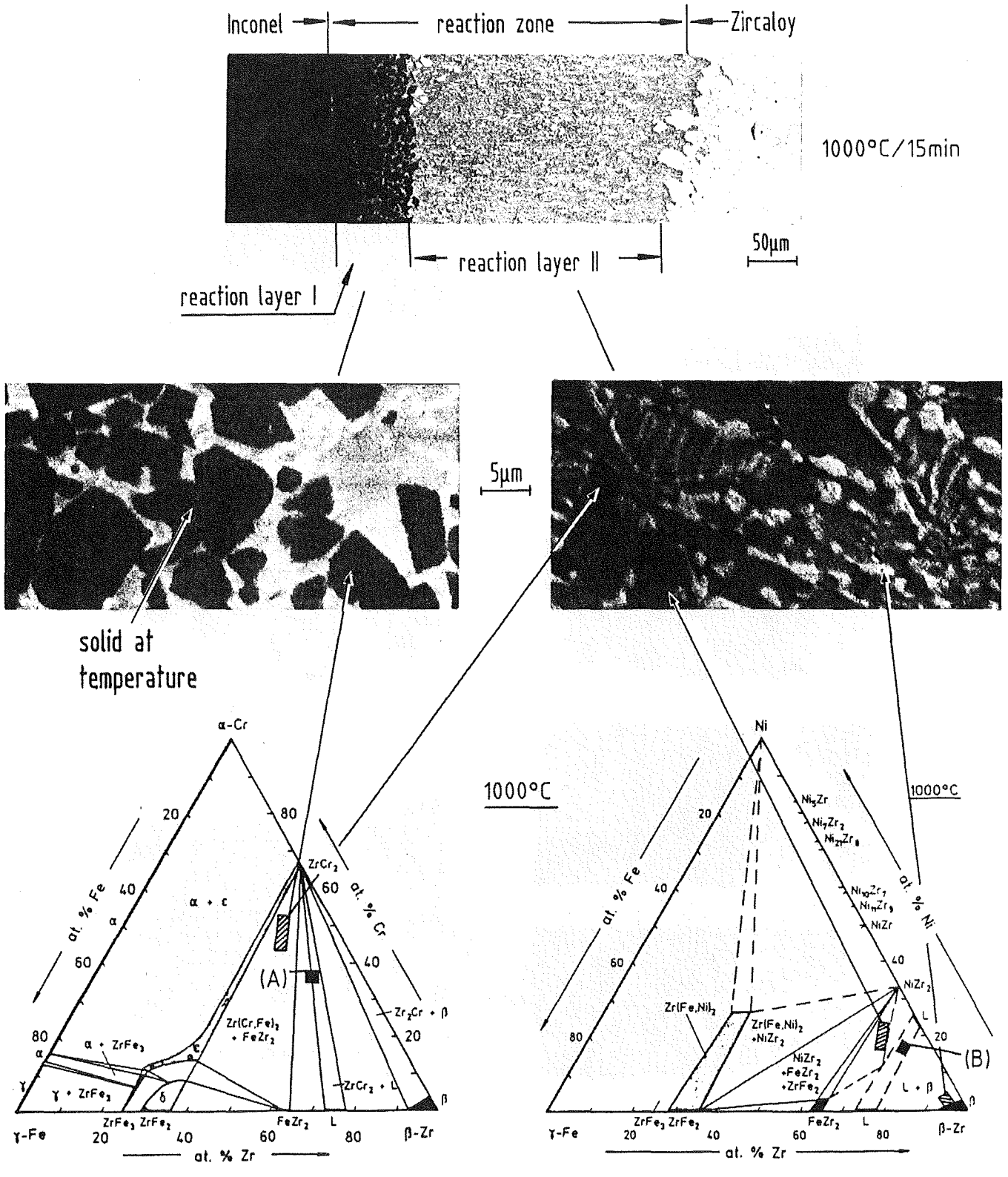

(A): integral analysis of reaction layer I

(B): integral analysis of reaction layer II

Fig. 12: Isothermal section of the Fe-Zr-Ni and Fe-Zr-Cr system at 1000°C [7]. Relation between the observed microstructures and the phase diagrams (Table 1).

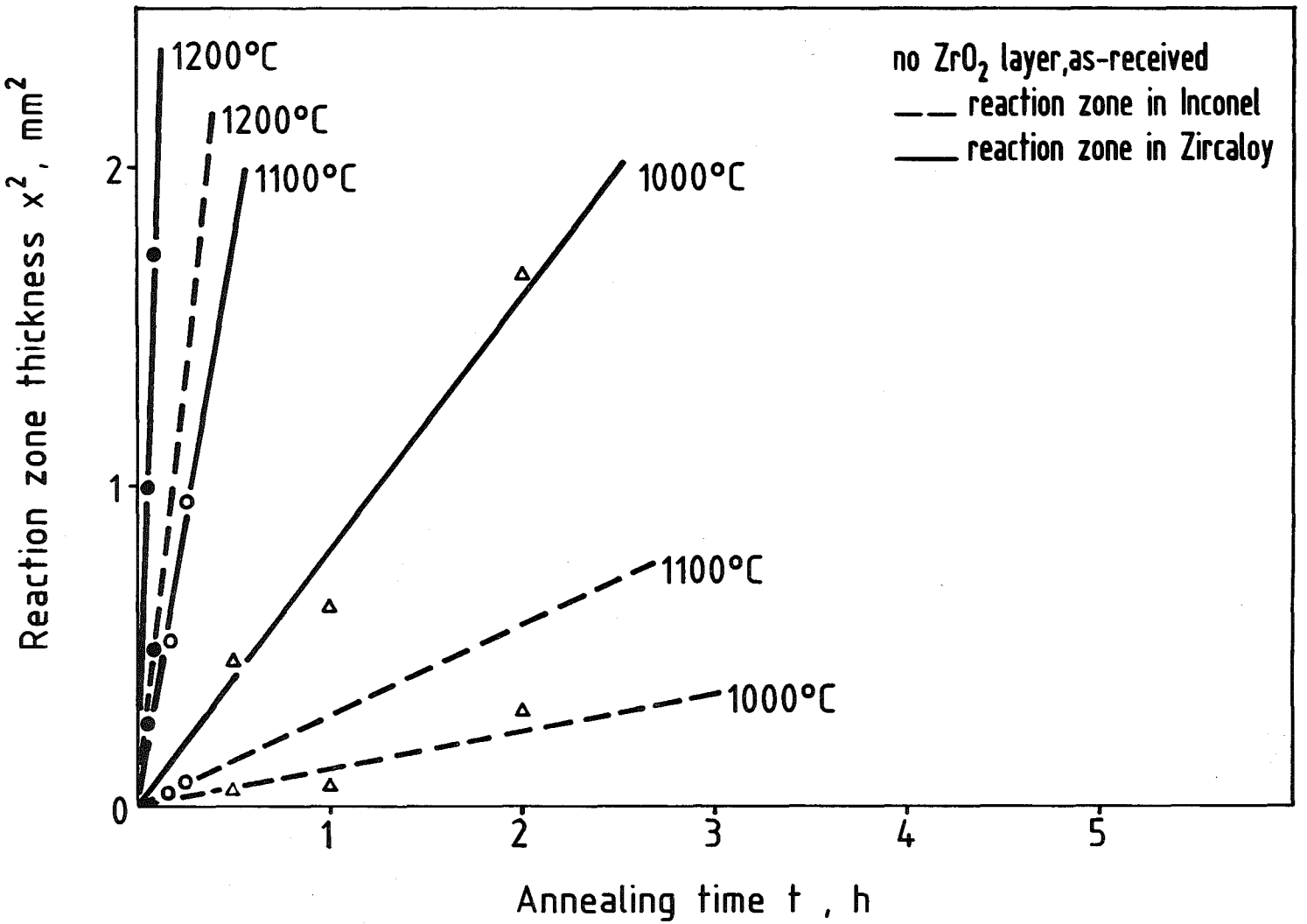

Fig. 13: Maximum reaction zone thicknesses in Zircaloy and Inconel for the Zircaloy-4/Inconel 718 system between 1000 and 1200°C (Table 2).

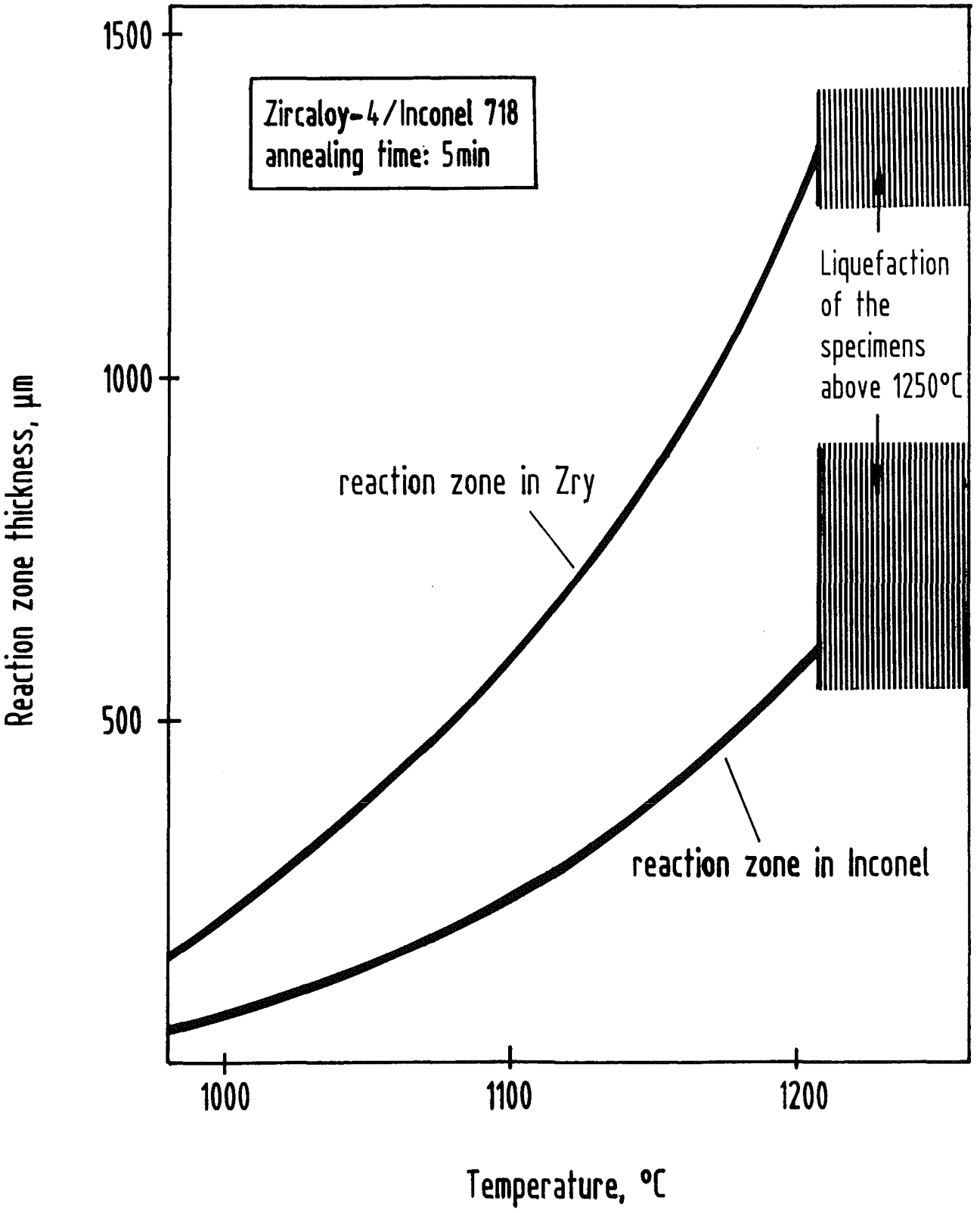

Fig. 14: Comparison of the reaction zone thicknesses in Zircaloy and Inconel for the Zircaloy-4/Inconel 718 system versus temperature; annealing time: 5 min.

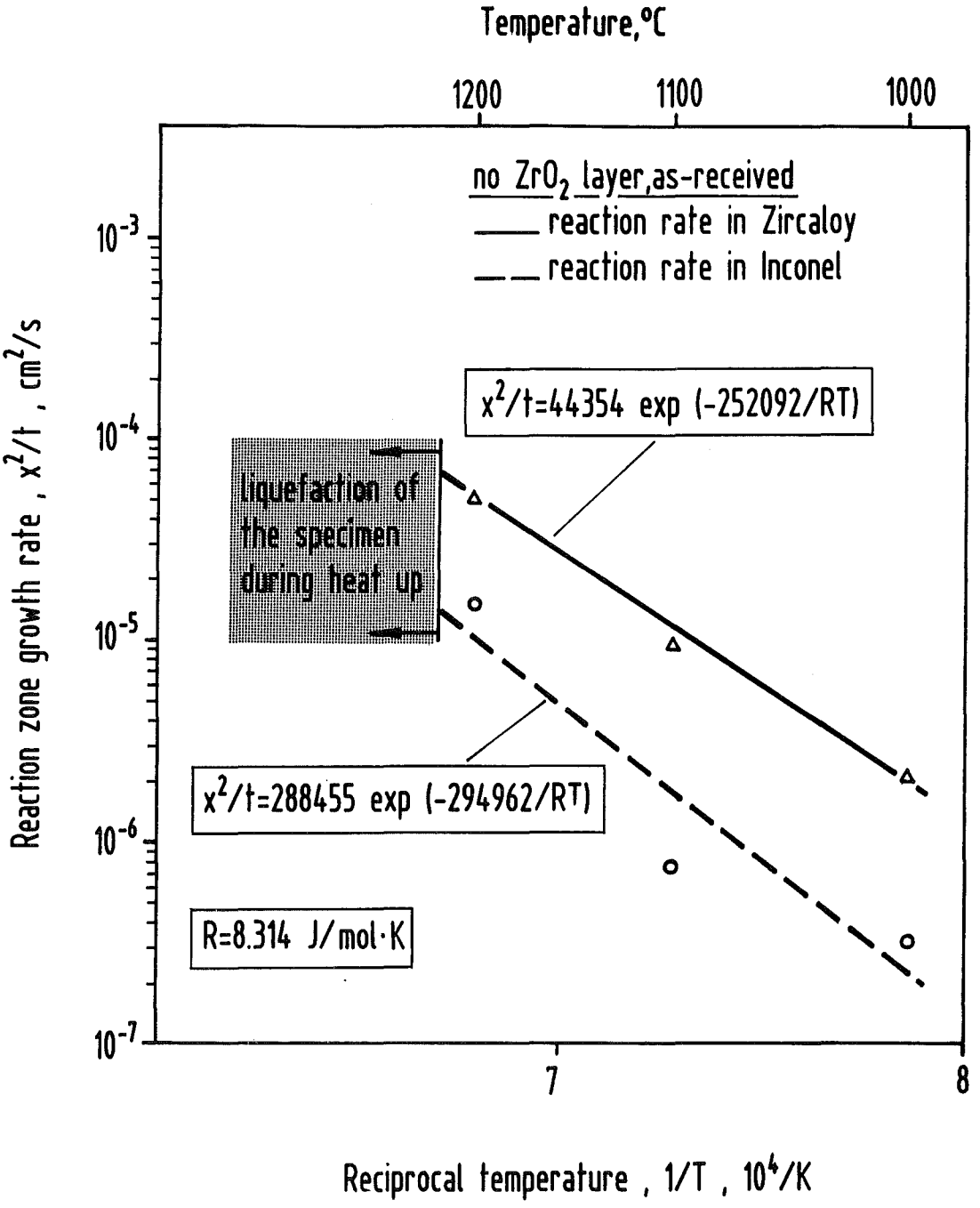

Fig. 15: Reaction zone growth rates for the Zircaloy-4/Inconel 718 reaction system (Table 3).

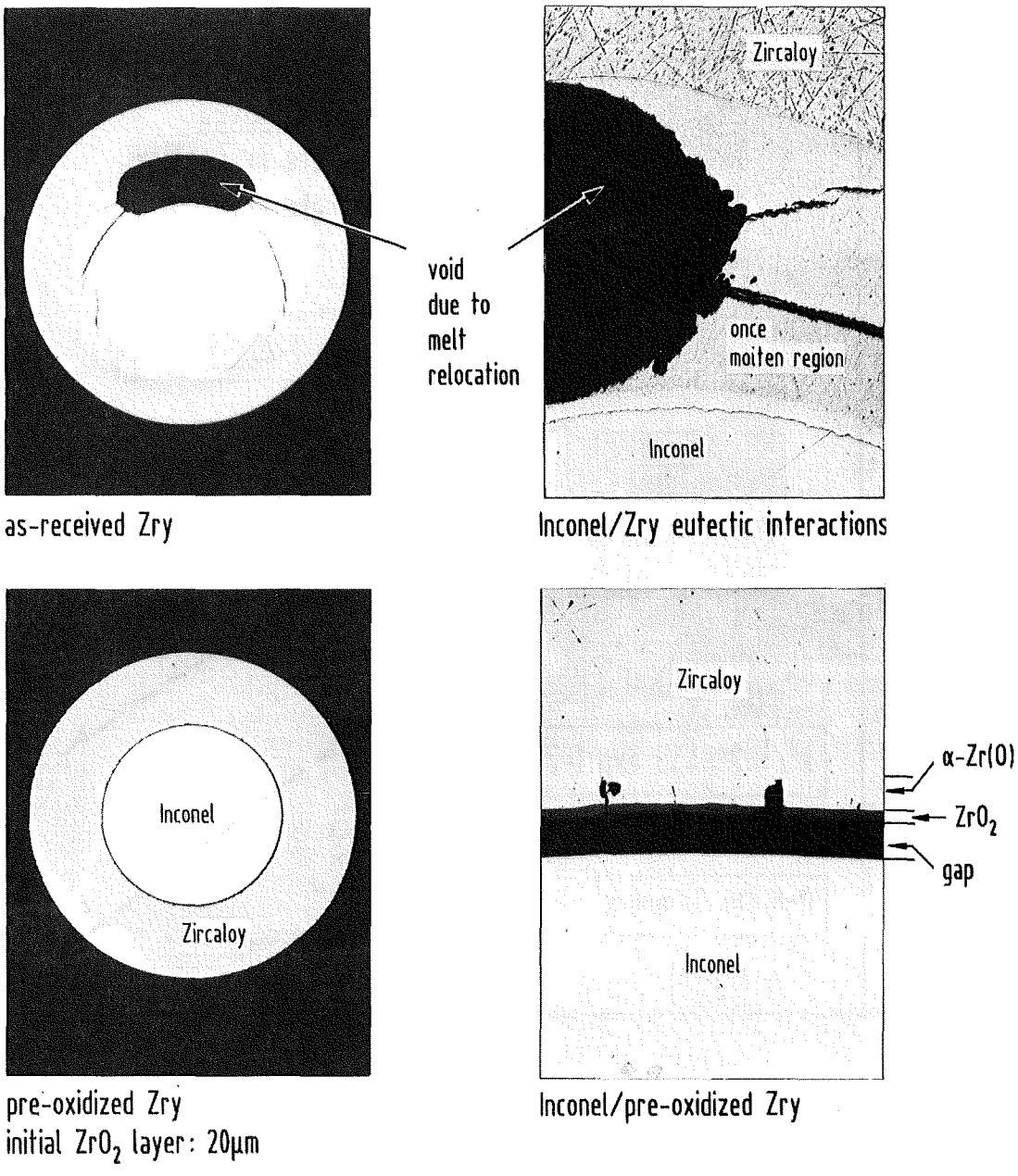

Fig. 16: Chemical interactions between Zircaloy-4 and Inconel 718; 1000°C/30 min. Influence of a 20 μm thick ZrO_2 layer.

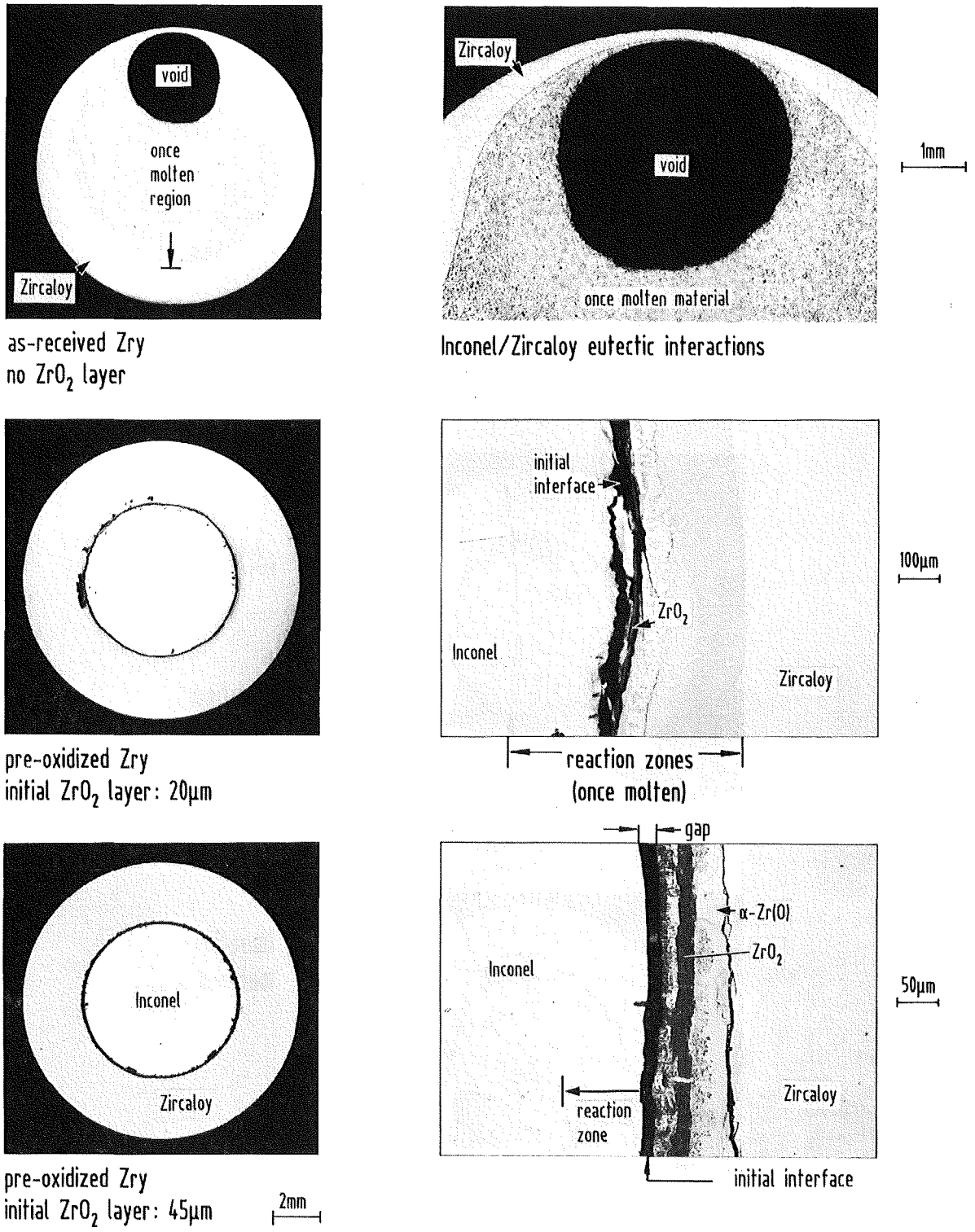

Fig. 17: Chemical interactions between Zircaloy-4 and Inconel 718; 1200°C/5 min. Influence of ZrO_2 layers of different thicknesses.

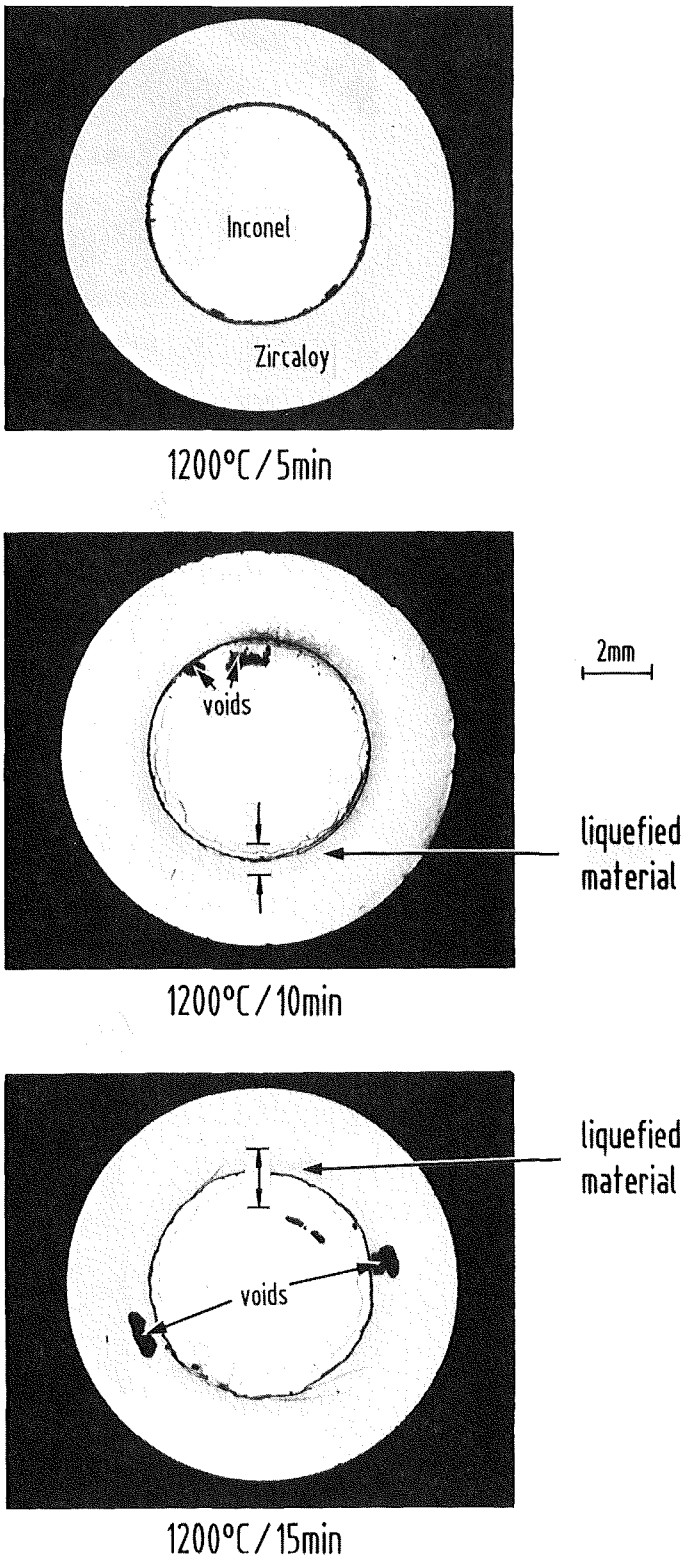

Fig. 18: Chemical interactions between pre-oxidized Zircaloy-4 and Inconel 718 as a function of time.

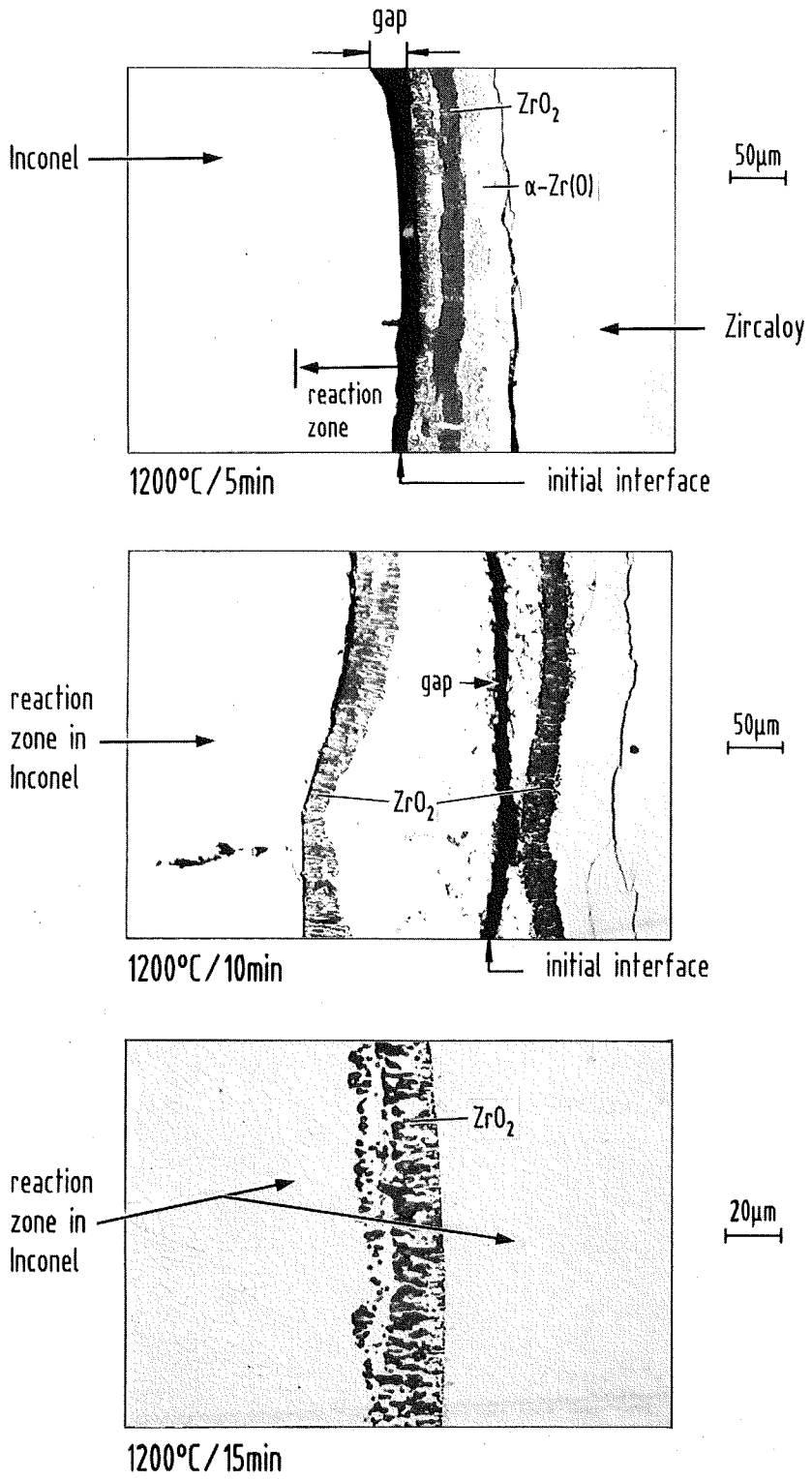

Fig. 19: Chemical interactions between pre-oxidized Zircaloy-4 and Inconel 718 as a function of time.

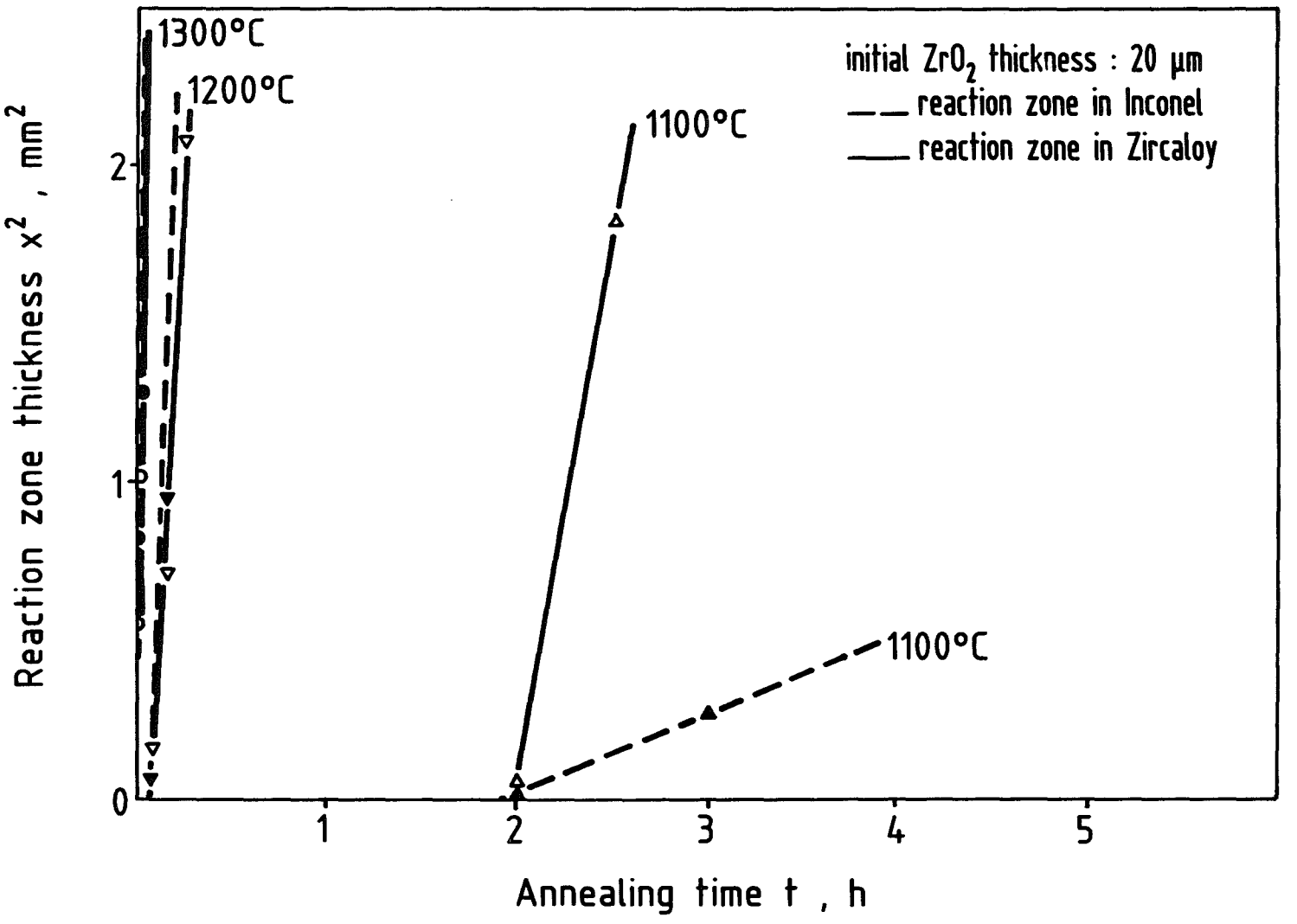

Fig. 20: Maximum reaction zone thicknesses in Zircaloy and Inconel for the pre-oxidized Zircaloy-4/Inconel 718 systems; initial ZrO_2 layer thickness: 20 µm (Table 4).

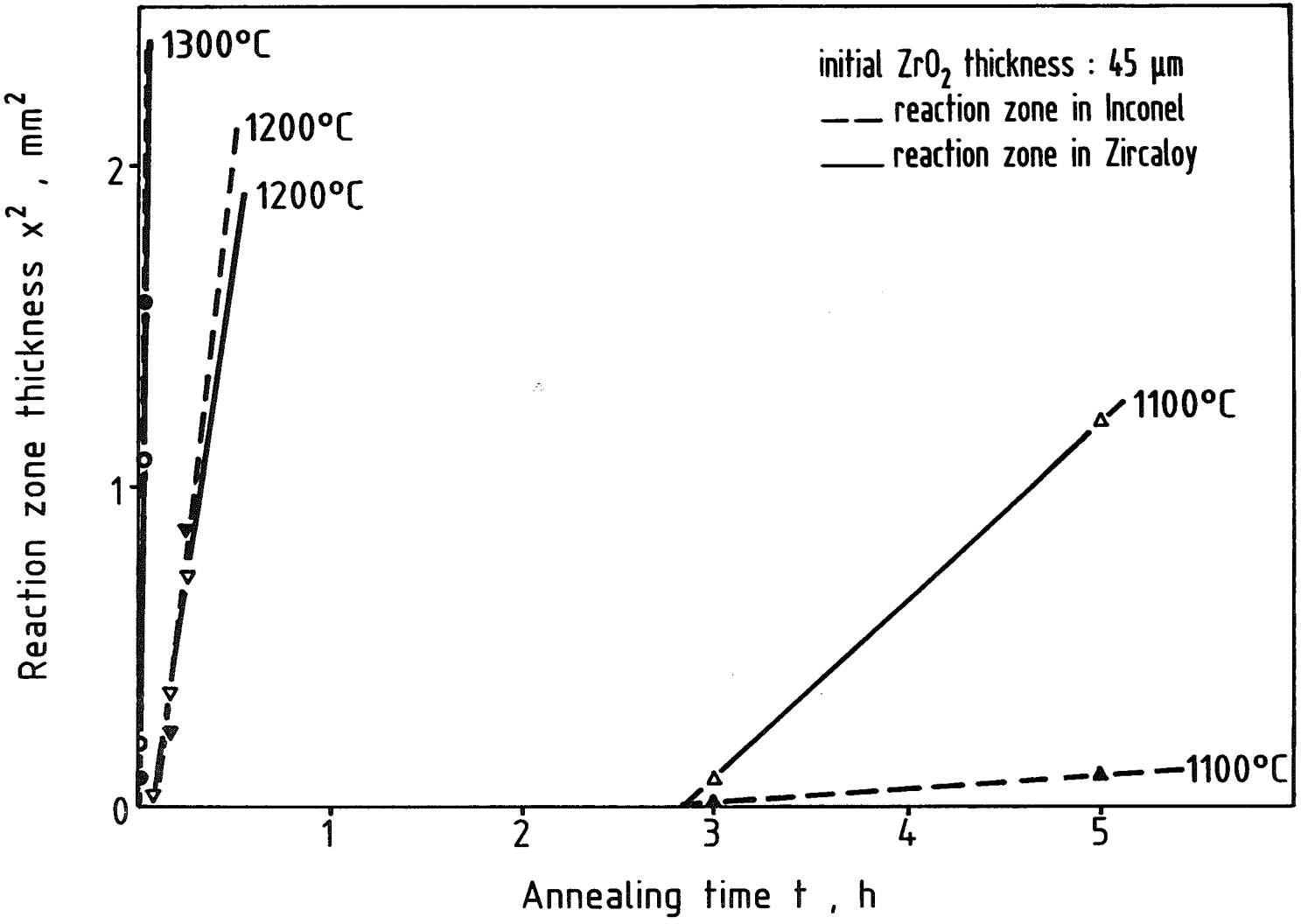

Fig. 21: Maximum reaction zone thicknesses in Zircaloy and Inconel for the pre-oxidized Zircaloy-4/Inconel 718 system; initial ZrO_2 layer thickness: 45 µm (Table 5).

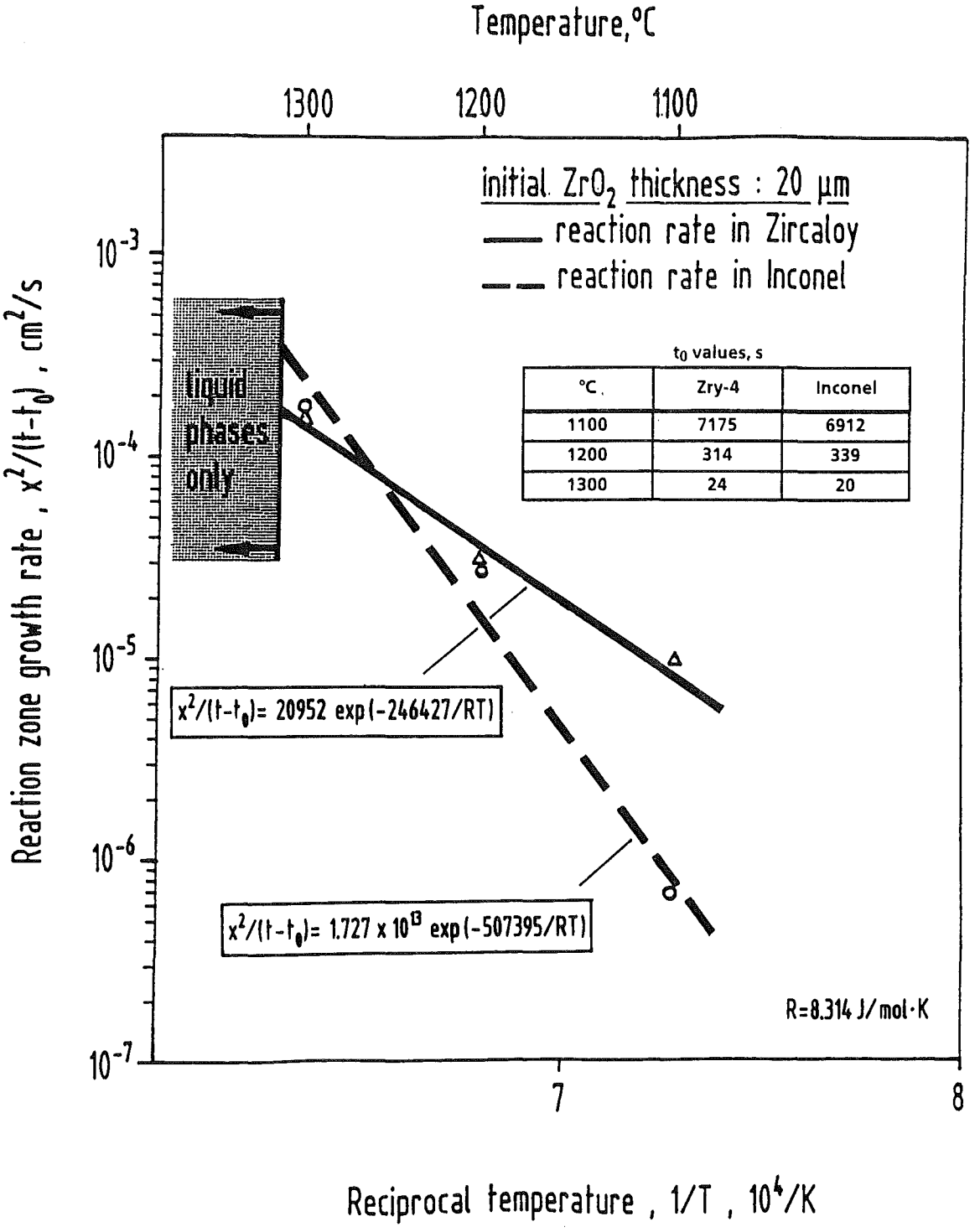

Fig. 22: Reaction zone growth rates for the pre-oxidized Zircaloy-4/Inconel 718 system; initial ZrO_2 layer thickness: 20 µm (Table 6).

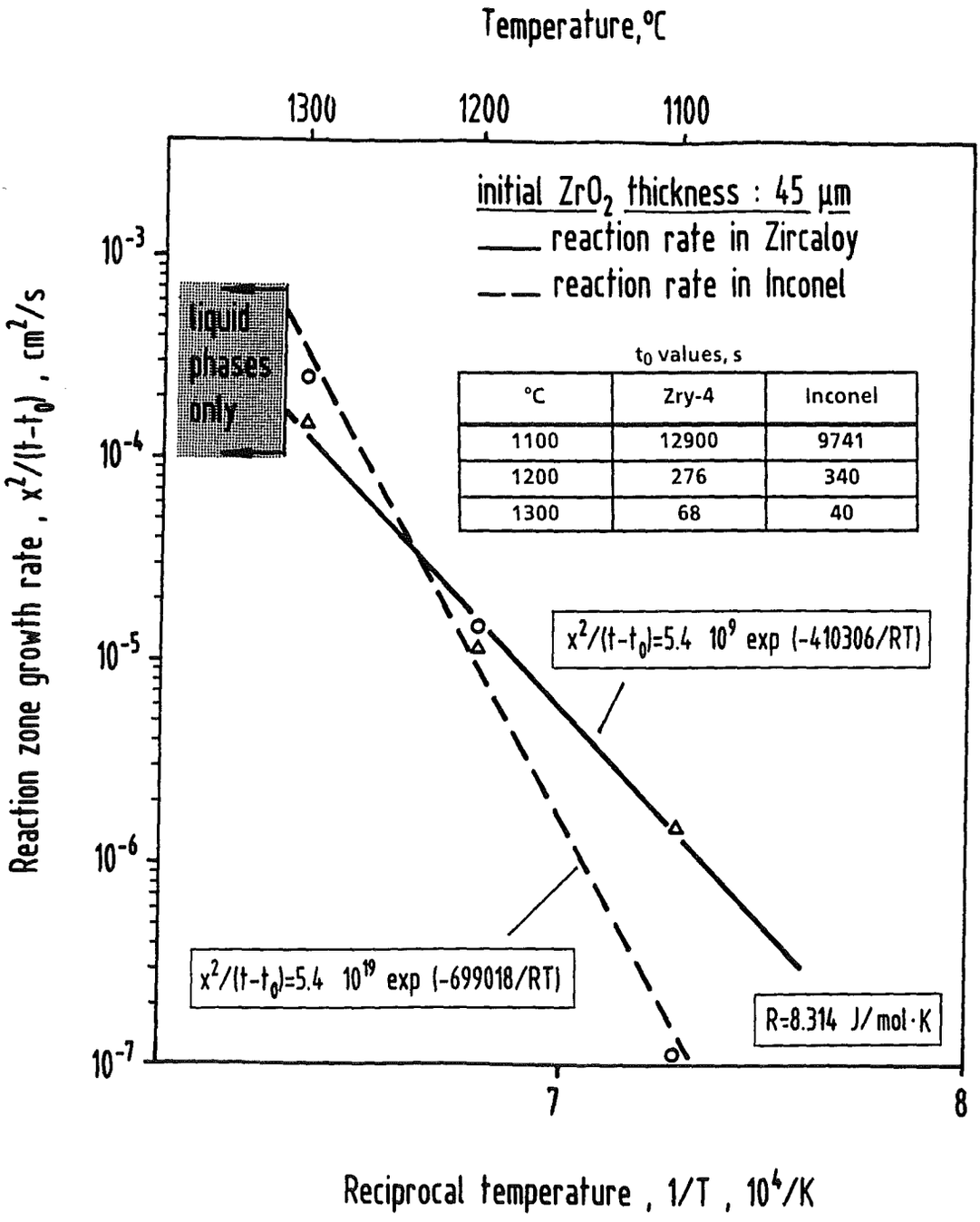

Fig. 23: Reaction zone growth rates for the pre-oxidized Zircaloy-4/Inconel 718 system; initial ZrO_2 layer thickness: 45 µm (Table 7).

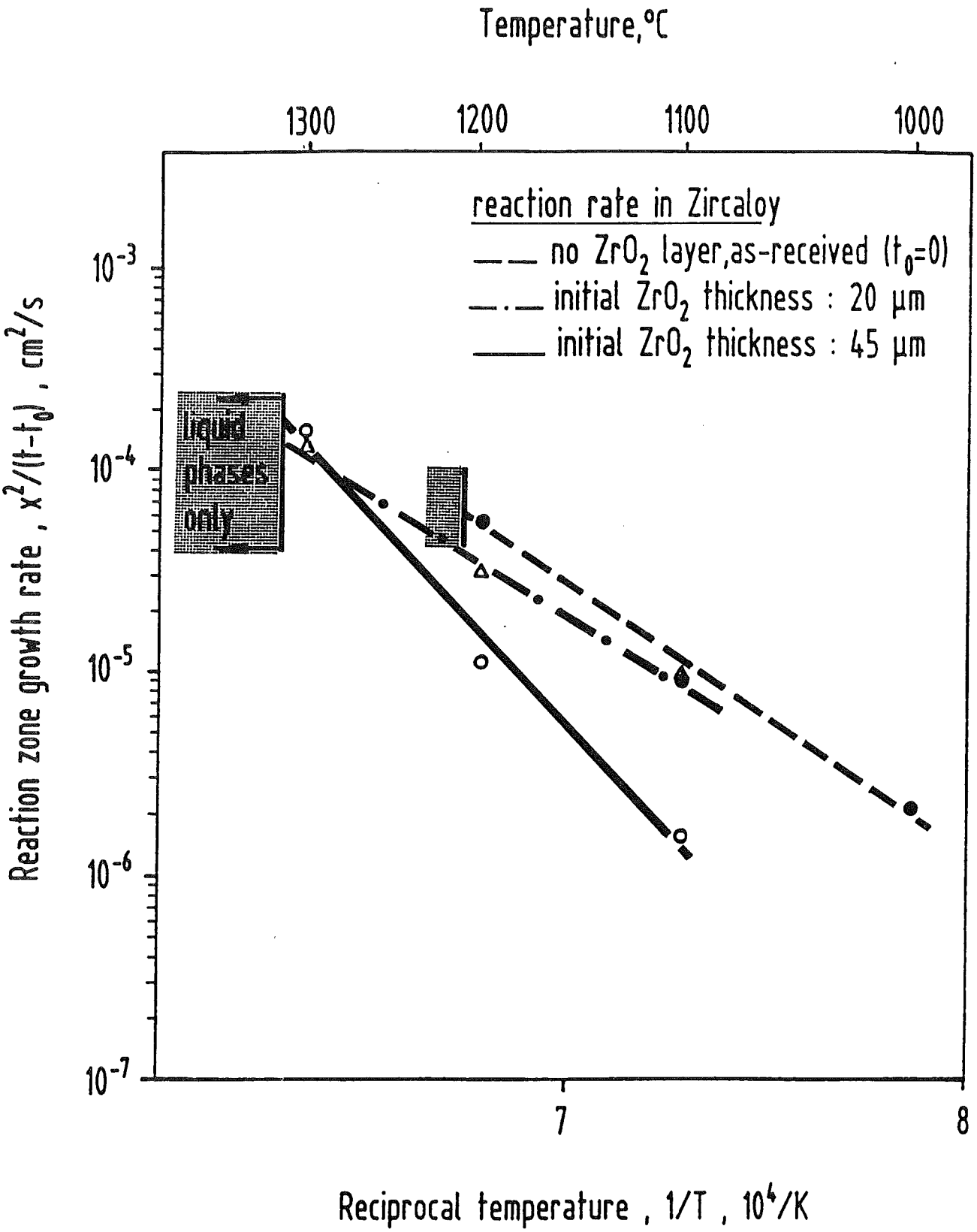

Fig. 24: Reaction zone growth rates in Zircaloy for the as-received and pre-oxidized Zircaloy-4/Inconel-718 system; influence of ZrO_2 layer thickness on reaction rate.

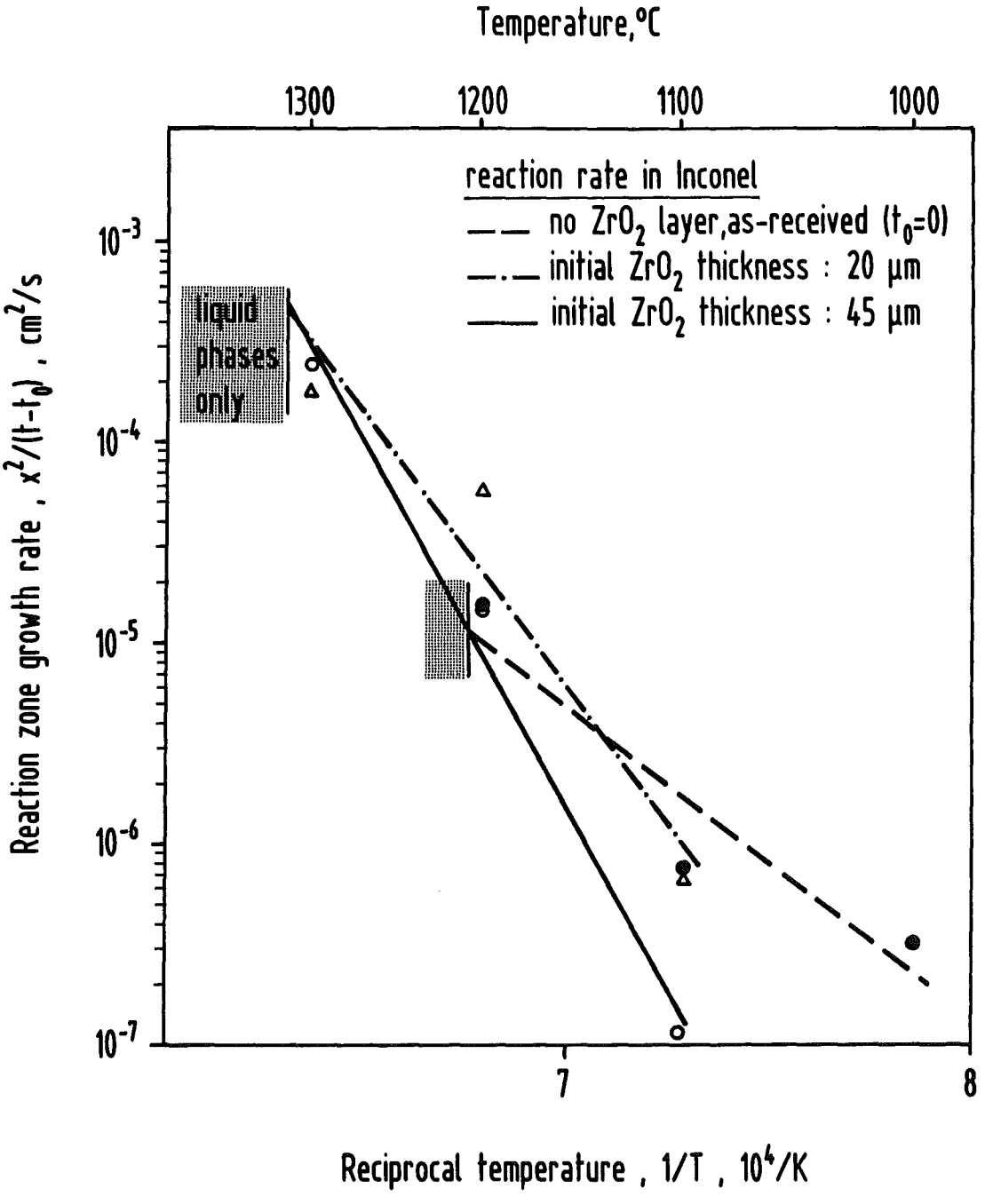

Fig. 25: Reaction zone growth rates in Inconel for the as-received and pre-oxidized Zircaloy-4/Inconel-718 system; influence of ZrO_2 layer thickness on reaction rate.

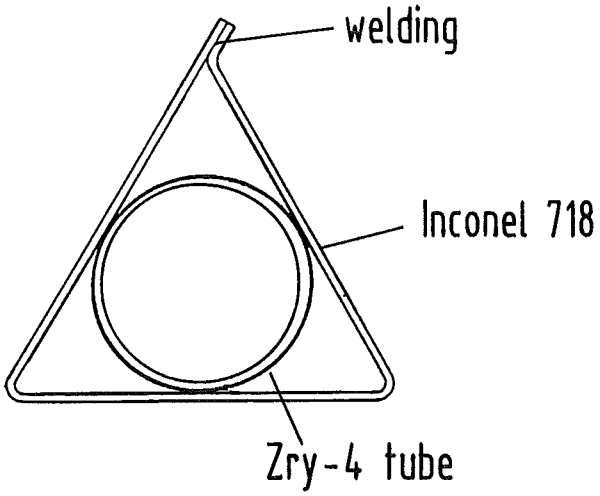

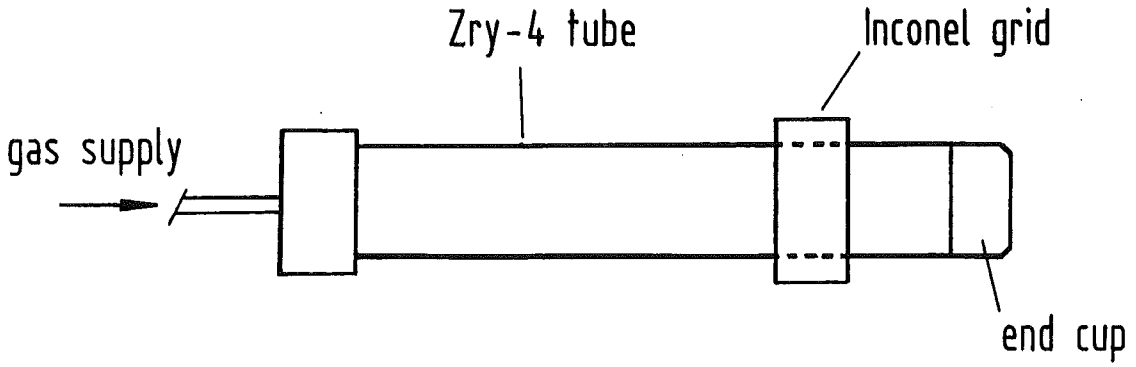

Fig. 26: Schematic of the Zircaloy-4 tube/Inconel 718 grid system spacer used in experiments under oxidizing conditions (steam).

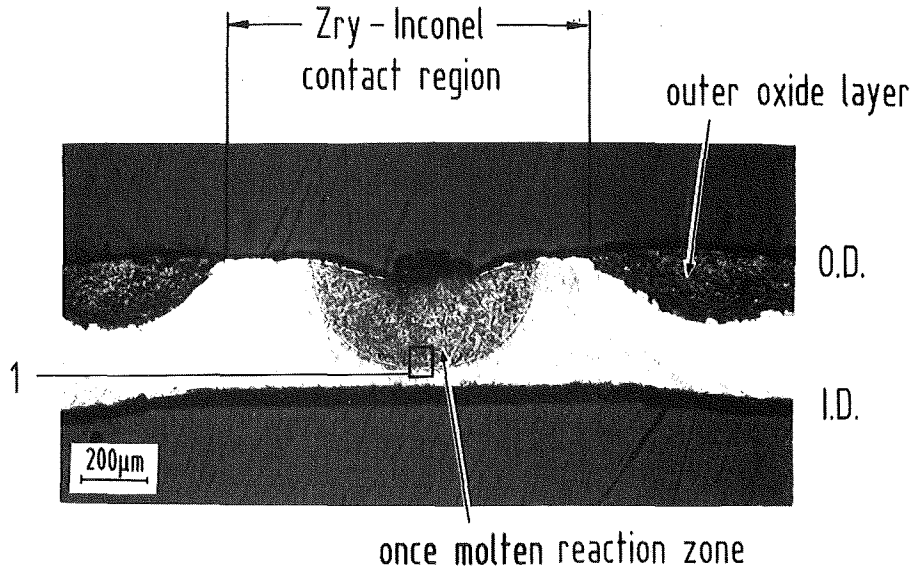

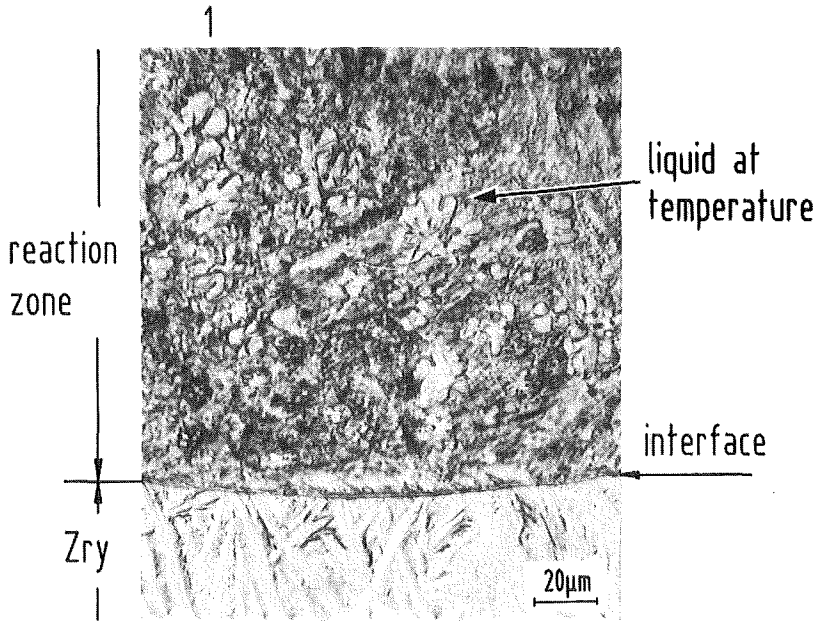

1150°C/3min

steam environment

Fig. 27: Chemical interactions between Zircaloy-4 tube and Inconel 718 after 3 min at 1150°C in steam atmosphere.